Environmental Fluid Mechanics **1:** 107–164, 2001.

Urban Fluid Mechanics: Air Circulation and Contaminant Dispersion in Cities

H.J.S. FERNANDO[a], S.M. LEE[a], J. ANDERSON[a], M. PRINCEVAC[a], E. PARDYJAK[a,b] and S. GROSSMAN-CLARKE[a]
[a]*Environmental Fluid Dynamics Program, Department of Mechanical & Aerospace Engineering Arizona State University, Tempe, AZ 85287-9809, U.S.A.*
[b]*Los Alamos National Laboratory, TSA-4, P.O. Box 1663, MSF 604, Los Alamos, NM 87545, U.S.A.*

Received 1 November 2000; accepted in revised form 22 November 2000

Abstract. Recently, many urban areas of the world have experienced rapid growth of population and industrial activity raising concerns of environmental deterioration. To meet challenges associated with such rapid urbanization, it has become necessary to implement wise strategies for environmental management and planning, addressing the exclusive demands of urban zones for maintaining environmental sustainability and functioning with minimum disruption. These strategies and related public policy must be based on state-of-the-science tools for environmental forecasting, in particular, on mathematical models that accurately incorporate physical, biological, chemical and geological processes at work on urban scales. Central to such models are the mechanics of environmental fluids (air and water) and their transport and transformation characteristics. Although much progress has been made on understanding environmental flow phenomena, a myriad of issues akin to urban flow, the transport phenomena, air and water quality and health issues (epidemiology) remain to be understood and quantified. We propose to initiate a new focus area – Urban Fluid Mechanics (UFM) – tailored to research on such issues. For optimal societal impact, UFM must delve into fundamental and applied fluid flow problems of immediate utility for the development of urban public policy and environmental regulations. Such efforts often entail the use of 'whole' systems approach to environmental studies, requiring careful synthesis between crosscutting areas.

In this paper, a few topics in the realm of UFM are presented, the theme being the flow and air quality in urban areas. Topics such as the scales of flow, the atmospheric boundary layer, pollutants and their transport and modeling of flow and air quality are briefly reviewed, discussed and exemplified using case studies. Identification of important flow-related issues, rigorous multidisciplinary approaches to address them and articulation of results in the context of socio-political *cause calebre* will be the challenges faced by UFM.

1. Introduction

Human communities have a tendency to pool in larger and more complex urban settings, with their environment being sensitively determined by complex interactions between a multitude of processes that span a myriad of scales. In the U.S., nearly two thirds of the population occupies less than 2% of the landmass, with a population density on the order of 1000 km^{-2} (Carbone, 2000). With the continued increase of population density in urban areas relative to their rural counterparts, it has become necessary to introduce a new paradigm of environmental prediction wherein the practice of 'uniformity of service', which commonly equates one

forecast per forecasting zone and relatively uniform geographic distribution of observing systems, be changed to a system based on the 'functionality' of the zone in point (Dabberdt *et al.*, 2000). Amongst the most functional and utile areas that need exclusive forecasts are the urban zones, being most vulnerable to heavy losses of property and life during environmental hazards. Urban environmental forecasting must include weather (temperature, humidity, winds), air quality (pollution levels), water resources, water quality and hazardous events (haze, fog, ice, floods, lightning), which are key ingredients for better managing and utilizing the Earth's environment to ensure sustainability and quality of life. An indispensable tool for environmental forecasting is predictive modeling, which largely relies on fluid mechanical principles governing transport, mixing and transformation phenomena in environmental fluids (air and water).

Considering the importance, extensity of scales and processes and the paucity of understanding of flow and transport phenomena of urban zones, it seems appropriate to introduce a new focus area within the environmental fluid mechanics – *Urban Fluid Mechanics (UFM)*. Fundamental and applied research underpinning the forecasting, management and planning of urban airsheds and watersheds will be central to UFM. The knowledge so created is expected to reduce scientific uncertainties on urban flow and transport issues of socio-political importance, thus contributing to the development of wise and ethical public policy. In the U.S., the national-level emphasis on urban zones is well articulated in the Clinton-Gore 'Livability' initiative (2000), which calls for new avenues to help urban communities to engage in such activities as ensuring clean air and water, preserving green space, easing traffic congestion and pursuing 'regional' smart growth strategies. The US National Academy of Engineering (NAE) has also initiated an extended dialog on 'Earth Systems Engineering (ESE)' to explore multidisciplinary issues akin to rapid urbanization in the coming decades.

The issues to be addressed by UFM are pervasive and hence cannot be covered by a single article. Therefore, this paper is focused on a set of selected topics related to urban air flow and air quality, which span a range of scales from synoptic- to nano-scales. The former signifies large-scale meteorological forcing and events ($>$1000 km) and the latter deals with particulate matter (PM; 0.001–10 μm) inhaled and transported to the lungs through human airways causing health problems (Oberdorster *et al.*, 1995). The intermediate (traditional meteorological) scales of interest are the meso [10 km–1000 km, with meso-α ($>$100 km), β ($\sim$100 km) and γ ($<$100km)] and micro [1 m–10 km, with micro- α ($>$100 m), β ($\sim$10 m) and γ ($\sim$1 m)] scales. The 'urban' scales (1 m–100 km) span cities and their suburbs, encompassing the so-called neighborhood (10 m–1 km), urban canyon/roadway ($\sim$10 m) and human (1 cm–1 m) scales. Fluid mechanical processes of these scales are complex, and they become even more complex in the presence of intricate boundaries (e.g., land and water) and chemical, biological, geological and physical transformations and processes of various length and time scales. Yet, public policy

on environmental issues is based on scientific understanding of such processes, especially on their integral effects over all scales.

An example is the distribution of contaminants in urban airsheds. The local flow therein is determined by the interaction between synoptic and meso-scale flows, terrain and landuse. Contaminants and their chemical precursors released from various sources are transported by the flow, turbulently mixed and subjected to chemical (e.g., ozone and secondary aerosol formation) and physical (coagulation, phase changes, deposition) transformations. These pollutants are distributed within the airshed by the flow, at times generating pollution hot spots (highly localized areas of extreme pollutant concentrations, typically <10 km), which can be (and has been) correlated with significant increase of health problems (O'Rourke *et al.*, 1993). Assessment of health risks associated with excessive exposure to pollutants is central to the development of air quality regulations and monitoring protocols.

Habitats of humans and other forms of life (the 'biosphere') are located within the atmospheric boundary layer (ABL), the study of which is of key importance in UFM. The nature of the urban ABL is largely dependent on the local terrain, land use and background flow conditions. Some examples are the smooth-flat terrain ABL (Figure 1(a)), urban flat terrain ABL (Figure 1(b)), which can be treated as a warmer, non-uniform roughness perturbation to the rural ABL and complex-terrain ABL (in areas replete with mountains, surface roughness, valleys and escarpments; Figures 1(c) and 1(d)). The latter is of particular interest, since major urban centers located along waterway transportation corridors are typically associated with complex terrain. It is also the least understood ABL of all. The urban fringe between the rural and urban areas is a zone of rapid changes (Figure 1(d)), rich in unsteady and non-equilibrium phenomena.

Section 2 will discuss aspects of urban boundary layers, paying attention to unresolved UFM issues at hand. Section 3 presents an introduction to urban air quality, noting the types of regulated pollutants and their transport in the urban ABL, which is further explicated in Section 4 by considering some case studies. Modeling of urban airflow (of various urban scales) and air quality are described in Section 5. A brief discussion of epidemiological studies is given in Section 6, and the expectations of UFM research are epitomized in Section 7.

2. The Atmospheric Boundary Layer

The ABL is the lower part of the troposphere that is directly influenced by the Earth's surface and responds to surface forcing with a time scale of about one hour or less (Stull, 1988). The flow therein can be driven by the pressure gradients (e.g., synoptic flow), surface heating (free convection) or heating/cooling of uneven terrain (slope flows). Over the land surface, the structure of ABL is strongly influenced by the albedo (which controls the solar input), roughness, surface emissivity, availability of water (evaporation) and heat capacity through their roles in determining the surface temperature and hence turbulent and radiative heat fluxes.

Figure 1. (a) A relatively 'smooth' flat terrain area (US Army Dugway Proving Grounds). (b) A typical urban flat terrain (Szeged, Hungary). (c) A developed urban area located in complex terrain (San Francisco). (d) A developing urban area located in complex terrain (Phoenix; courtesy of Ramon Arrowsmith). Note the urban fringe separating the developed and completely undeveloped areas.

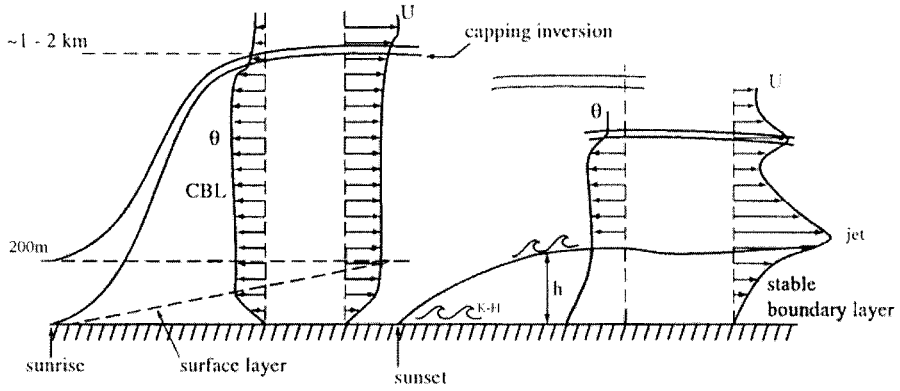

Figure 2. The development of ABL over flat terrain. The potential temperature θ and wind velocity U are shown for the convective (CBL) and stable (SBL) boundary layers. Note the development of the CBL following sunrise and the response of the existing capping inversion zone aloft. Following sunset a ground-based inversion layer develops, leaving a residual inversion above.

It is customary to divide the ABL into several layers (Figure 2), a *surface layer* of depth 50–100 m where the shear stress is approximately constant and a region above up to 500–1000 m where the shear stress is variable and the flow is influenced by surface friction and Earth's rotation. At greater heights the flow is geostrophic. Other regions of dynamical importance are defined as needed, depending on the nature of the boundary layer. Scores of dominant flow configurations are possible, and hence a rigorous classification of ABLs is not possible. Yet a broad classification useful for UFM studies can be proposed based on terrain characteristics, and the following discussion revolves around such a classification.

2.1. FLOW AND TRANSPORT IN FLAT TERRAIN ABL

2.1.1. *Uniform Terrain*

This is the simplest category of ABL, with the most studied case being that over a flat, smooth surface for which theoretical analyses can be advanced assuming horizontal homogeneity of turbulent fields (Arya, 1999). The case of uniform roughness has also received considerable attention (Macdonald, 2000). In nature, however, the case of homogeneous terrain is the exception rather than the norm. Comprehensive field observations (Kaimal, 1972; Kaimal *et al.*, 1976), laboratory experiments (Deardorff *et al.*, 1969, 1980; Snyder *et al.*, 1990; Piper *et al.*, 1995; Cole and Fernando, 1998), numerical modeling (Deardorff, 1970; Moeng and Wyngaard, 1984; Galmarini *et al.*, 1998) and similarity theory (for reviews, Kaimal and Finnigan, 1994; Mahrt, 1998) have contributed much to our understanding on these boundary layers. Homogeneous terrain studies have been excellent precursors for understanding and modeling more complex situations such as urban boundary layers.

As shown in Figure 2, following sunrise, the convective boundary layer (CBL) develops due to heating of air adjacent to the ground, and grows during the day while destroying the stable stratification of the prevailing layer aloft. The growth, and hence vertical transport, of the CBL is governed by convective turbulence as well as by the entrainment at the capping inversion bounding the CBL. Steepest gradients of the wind speed and its direction as well as temperature occur in the bottom 10% of the CBL: in the middle of CBL strong convective mixing smoothes out all vertical variations of the mean profiles. The scaling for turbulence and concentration fluctuations in the CBL are fairly well understood (Deardorff, 1970, 1985; Kaimal *et al.*, 1976; Petersen *et al.*, 1999), though some details of transport mechanisms of heat and tracers through them still remain unresolved (Siggia, 1994).

The decrease of heat flux in the afternoon leads to concomitant weakening of the turbulent intensity, but the decay is rapid immediately prior to sunset due to damping of feeble eddies by the overlying inversion (Caughey *et al.*, 1979; Nieuwstadt and Brost, 1986; Grant, 1997; Sorbjan, 1997; Cole and Fernando, 1998). This transition is characterized by the appearance of one or more shallow inversion layers beneath the capping inversion and the development of a stable ground-based nocturnal inversion (SBL). The top of the SBL is not as sharply defined as the top of the CBL. Turbulence levels in the SBL decrease gradually with height, damped out by static stability. A rich variety of processes, such as low level jets, meandering motions, Kelvin-Helmholtz instabilities, heat and radiative flux divergences and gravity waves characterize the SBL. Lacking a mechanism to induce significant mean vertical motions, vertical transport in the SBL is mainly realized by turbulence (Hunt, 1985; Coulter, 1990; Nappo, 1991; Weber and Kurzeja, 1991; Fernando and Hunt, 1996). Since the vertical displacements of fluid parcels in stratified turbulence are constrained by the buoyancy length scale $L_b = \sigma_w/N$, where σ_w is a characteristic (r.m.s.) vertical velocity and N is the buoyancy frequency (Hunt, 1985; Hunt *et al.*, 1985), the vertical transport and mixing in the SBL are weak and pollutants tend to be trapped therein. The evening and morning transitions from CBL to SBL and *vice versa* remain poorly understood and inadequately parameterized in models, and hence most meteorological models fail dramatically during transition periods. However, in urban areas, these are precisely the periods where their accurate performance is needed the most, to assess the build up of pollution during morning and evening rush hours.

It is instructive to classify SBLs based on the degree of 'stability,' quantified by a suitably defined gradient Richardson number $Ri_g = N^2/(\partial \bar{U}/\partial z)^2$, where $\partial \bar{U}/\partial z$ is the mean velocity shear. The case of $Ri_g > 1$ is called the very stable boundary layer, characterized by light winds, layered structure and intermittent turbulence wherein Monin–Obukhov theory is invalid (Mahrt, 1998). In the weakly stable case ($0.25 < Ri_g < 1$), on the other hand, significant winds maintain more or less continuous turbulence, describable by the Monin–Obukhov theory. Alternative classification schemes have also been used with equal success (Mahrt, 1998;

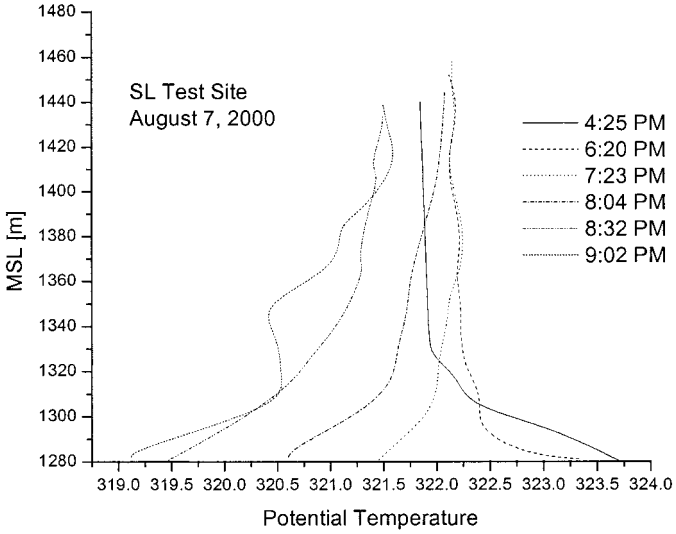

Figure 3. The development of the stable stratification over the flat relatively smooth terrain at the SLTEST site. The vertical axis represents the height above the mean sea level.

Derbyshire, 1990; Holtslag and Nieuwstadt, 1986). It should be noted that, despite much recent progress, the understanding of the SBL is not nearly as complete as the CBL (Malhi, 1995; Derbyshire, 1995a,b; Oyha *et al.*, 1997; Mahrt, 1998). This has motivated a recent multi-agency field study CASES-99 (Cooperative Atmospheric Surface Exchange Study) carried out in Kansas during October 1999.

A special facility (SLTEST) has been recently constructed at the U.S. Army Dugway Proving Ground to study the flat-terrain 'smooth' boundary layers (Figure 1; Klewicki *et al.*, 1998). During a recent experiment at SLTEST (August 1–6, 2000), a tethered meteorological tower was used to suspend instruments up to 180 m above the ground level to measure the ABL development. Figure 3 shows the virtual potential temperature profiles taken at different times of the afternoon and evening. The profile at 4:25 PM reveals an unstable CBL. From 6:20 to 7:23 PM, significant cooling of the ground can be seen, thus forming the SBL, which continues until the sounding taken at 8:32 PM. At 9:02 PM, however, the stratification above 25 m is destroyed by the arrival of a jet-like flow originating at distant mountains and intruding at its equilibrium density level. This illustrates the difficulty of observing 'text-book' boundary layers in nature and the importance of dealing with multi-scale flow even in idealistic natural test beds.

A number of studies conducted using uniformly distributed artificial roughness elements have provided valuable information on the flow structure within and above roughness canopies (Macdonald, 2000). Such studies, although of great importance, provide only partial information on natural roughness such as vegetation. Plants are living organisms and the description of energy and mass fluxes between a vegetation-covered land surface and the atmosphere is complicated by biological

and biochemical processes. Vegetation is able to transpire and therefore dissipate a large fraction of the incoming radiation and turbulent energy into phase changes of water. The water fluxes are controlled by means of leaves' stomata (adjustable openings in the leaf surface) and hence are tightly coupled with CO_2 fluxes. Transpiration from plants can equal or exceed the evaporation rate from soils or even from open water, because of its vertical structure. Depending on the root depth, water might be available for a certain period of time under drought conditions. In comparison to soils, the energy and water stored in the canopy is easy accessible. If the soil surface is dry, its hydraulic conductivity decreases dramatically, making it difficult to access water from deeper soil layers.

The reflectance of leaves in the visible part of the spectrum is much lower than that of most soil surfaces, while the reflectance in the near-infrared region is generally much higher. Since each of these spectral regions carries about half of the total solar energy, both must be taken into account separately in the presence of vegetation. The long-wave emissivity of leaves is high (0.97–0.98) in comparison to that of soil (0.89–0.93). The aerodynamic characteristics of vegetation ought to be treated as roughness elements of porous and fibrous nature, not as bluff obstacles or smooth surfaces, except for very short vegetation (Brutsaert, 1979). The aerodynamic characteristics might change (sometimes within a day) due to adaptation of leaf-angles to immediate environmental conditions, because of seasonal cycle of leaf growth and fall or due to long-term natural growth. Owing to the very low heat-storage capacity of vegetation, almost all the absorbed solar radiation is partitioned between turbulent sensible and latent heat fluxes. Conversely, soil surfaces conduct heat into or receive from the deeper layers of the ground. Fluxes of trace gases through leaves' stomata are also affected by complex biochemical processes. The parameterization of such processes is a major challenge for urban ABL modeling.

The ABL over vegetation with unlimited water supply supports an increased latent heat flux compared to sensible heat flux, thus enhancing the entrainment of warm dry air from the capping inversion. As a result, the atmosphere above fully transpiring vegetation is somewhat similar to that above the sea. Figure 4 shows an example of the diurnal cycle of energy fluxes and canopy temperature for a well-irrigated, full-cover wheat canopy under semi-arid conditions. Note that the canopy temperatures of well-watered vegetation can be considerably lower than the air temperature for high vapor pressure deficits, which occur in the late afternoon (Idso, 1982). Under such conditions, latent heat fluxes can be higher than the absorbed solar radiation and sensible heat fluxes are directed toward the canopy.

Recently, an increasing number of feedback mechanisms have been included in vegetation-ABL studies (Jarvis and McNaughton, 1986; McNaughton and Jarvis, 1991; Jacobs and DeBruin, 1992; Dickinson *et al.*, 1997; Raupach, 1998), which show that physiological, aerodynamic and boundary layer feedbacks need to be considered in unison to understand surface energy and mass fluxes. On a larger scale, studies using simple models have shown that the development of the ABL

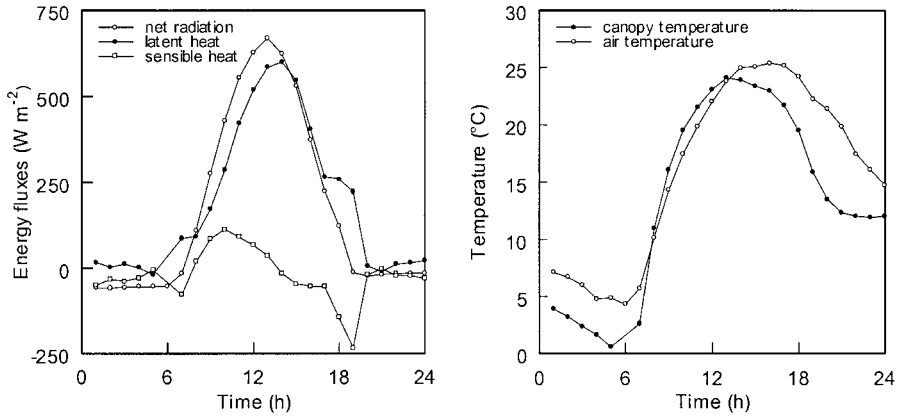

Figure 4. Data obtained on 15 April 1993 for a full-covered and well-watered spring wheat canopy during the Free-Air Carbon Dioxide Enrichment Experiment, Maricopa, Arizona, USA. The measurements and further results are described in Kimball *et al.* (1999). Relative humidity (RH) of the outside air in the afternoon hours was less than 25% and the canopy RH is close to saturation.

is controlled to a great extent by the water fluxes from a vegetated surface into the atmosphere (Avissar and Verstraete, 1990; Garratt, 1994).

In meteorological models, the interaction between natural land surfaces and atmosphere is described by means of Soil-Vegetation-Atmosphere-Transfer (SVAT) schemes. Typically, a horizontally homogeneous terrain is assumed, leading to spatially uniform vertical turbulent fluxes. If only the turbulent surface fluxes, not the micro-meteorological variables deeper in the canopy, are of interest then the plant canopy can be represented by a one-layer model built upon the so-called 'big-leaf' concept (Monteith, 1965; McNaughton and Jarvis, 1983), instead of using multi-layer models (Raupach and Finnigan, 1988; McNaughton and Jarvis, 1991). The 'big-leaf' is assumed to have the same aerodynamic and optical characteristics as the canopy, with all leaves within experiencing the same microclimate. The intercellular air spaces are water-saturated and the water vapor pressure is equal to the saturation pressure at the canopy temperature. The fluxes of energy and mass are obtained by gradient-flux relationships, which are combined with a logarithmic wind profile and stability functions. Extension of such modeling for sparse canopies has also been attempted (L'homme and Monteny, 2000). Higher-order closure models are theoretically superior, but have not improved the accuracy of simulations over those based on first-order representations (Avissar and Verstraete, 1990). The latter, however, are incapable of simulating detailed processes inside vegetation canopies such as thermal puffs or wind up-drafts.

Besides the development of averaging methods to represent sub-grid heterogeneity and horizontal water fluxes, recent improvements to SVAT models have been directed at understanding the dynamic changes of vegetation characteristics occurring on different time scales (IGPO, 1997). An example is the simultaneous

calculation of energy, water and CO_2-fluxes, with the aim of improving the accuracy of surface resistance calculations. This calculation is hinged on the observed strong correlation between the net CO_2 assimilation rate and stomatal resistance in leaves for a wide range of environmental conditions (Wong *et al.*, 1979), permitting substantial simplifications in model development. Net assimilation rate can be simulated by means of biochemical models (Farquhar and von Caemmerer, 1982) as a function of the absorbed solar radiation, leaf temperature, atmospheric CO_2 concentration and leaf nitrogen content. Much research has been focused on the spatial scaling from leaf to canopy level and pertinent temporal parameterizations (Amthor, 1994; Leuning *et al.*, 1995; De Pury and Farquhar, 1997; Wang and Leuning, 1998). Subsequent studies have shown that the models are able to simulate energy, water and CO_2-fluxes for different vegetation types and environmental conditions with a very high accuracy (Amthor *et al.*, 1994; Leuning *et al.*, 1998; Grossman-Clarke *et al.*, 1999).

Additional complexities arise when soil and vegetation surfaces coexist with different types of land use, which is typical in urban areas. In this case, an additional flux has to be introduced in the surface energy balance equation describing the anthropogenic release of heat due to combustion (also called 'urban respiration', Collins *et al.*, 2000). This energy source might supply a considerable amount of heat in some cities (Oke, 1987). As with other energy fluxes, it is subject to daily and seasonal changes; the anthropogenic flux component obviously depends on the population density, culture and economic status.

2.1.2. *Hetrogeneous Terrain*

Urbanization causes drastic changes in radiative, thermal, moisture and aerodynamic characteristics of the land surface (Oke, 1987), leading to hetrogeneities of the flow. In urban modeling, cities can be treated as whole units whose details are relatively unimportant or else the terrain within, such as isolated buildings and street canyons, can be treated in detail (Hosker, 1987; Ellefsen, 1993). In the former, only a little knowledge on the physical layout of the city is required, and integral effects of urban structure, vegetative elements and variable terrain are considered as perturbations to the background flow. Most models developed hitherto use this approach, such as those of Hanna (1975), Hanna *et al.* (1982), Johnson *et al.* (1976), Turner (1979) and Bornstein *et al.* (1996). Obviously, the second approach involves intensive computations of flow around numerous urban land use elements. Aerially integrated (satellite) views of urban surfaces together with measurements at representative sites (e.g., rooftop levels) are used to map such elements for modeling.

A schematic of a typical flat urban modeling domain is shown in Figure 5 (cf., Figure 1(b)). The Urban Canopy Layer (UCL) extends from the ground to about the roof level of buildings, and is strongly dominated by local site characteristics. It is in this area that the local flow and turbulence strongly affect the near-field dispersion of contaminants. The Urban Boundary Layer (UBL) occupies the area

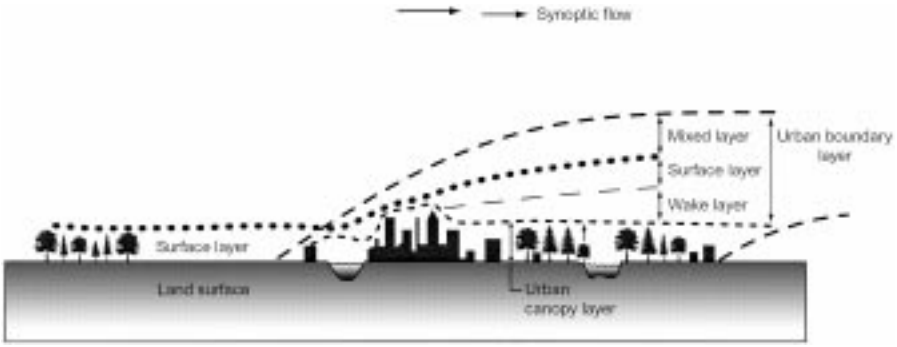

Figure 5. A typical urban domain over flat terrain.

from UCL to the level at which urban surface influence is no longer felt, which includes the turbulent wake layer (also called the internal boundary layer) immediately affected by the roughness elements, the turbulent surface layer, and the mixed layer. The UBL and UCL are key elements in predicting the modification of background (synoptic and meso-scale) winds by cities and in obtaining high-resolution local wind fields. Realizing the required coupling between these different layers is a major challenge for UFM.

The important roles of aerodynamic roughness and thermal inhomogeneities in determining urban wind fields have been recognized and studied for many decades (e.g., Kukharets and Tsvang, 1998). The elevated temperatures in cities arise due to anthropogenic heat generation from buildings, greater absorption of incoming short-wave radiation and reduction of outgoing long-wave radiation due to pollution in lower layers, and increase of sensible temperature due to reduced latent heat flux from non-porous urban surfaces such as pavements and roads (Oke, 1984, 1995). These factors can retard nocturnal cooling of urban surfaces between sunset and midnight, in contrast to rural surfaces that are cooled more rapidly, causing higher temperatures over the city relative to its vicinity (the Urban Heat Island effect; Bornstein and Oke, 1981, Hogan and Ferrick, 1997). In modeling, the urban heat island effect can be specified by an urban-rural temperature difference ΔT or by using a patch of enhanced heat flux (Baik and Chun, 1997). The strengths of inhomogeneities are determined by numerous factors such as morphology, latitude, and population. Temperature difference ΔT increases as high as 12 °C have been recorded in some North American cities, with values of up to 14 °C have been projected to occur by the year 2000 (Hunt, 1996).

The urban heat island effect may produce major temporal and spatial alterations to the thermodynamics and circulation of the urban ABL (Bornstein, 1987). The magnitude of the rural-urban temperature difference, ΔT, driving this circulation is dependent on a variety of factors including cloud cover, vegetation and wind speed. For example, clear skies allow strong rural cooling, and hence the development of larger ΔT, whereas strong winds reduce ΔT. Oke and Hannell (1970) have demonstrated the existence of a threshold wind speed U_c prohibiting the urban heat

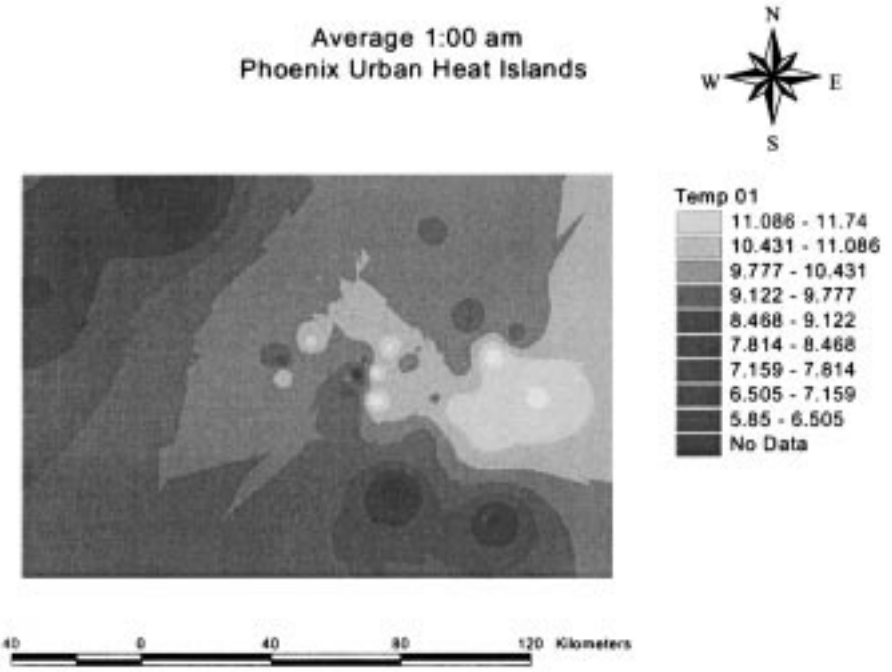

Figure 6. The urban heat island in the airshed of Phoenix, Arizona (USA). The surface level measurements collected by 44 surface stations operated by various public agencies were used to calculate the monthly average temperature (in °C) distribution between 1:00 to 2:00 A.M. during the month of January 1998.

island development, which is correlated to the population P (in millions) as $U_c = 3.4 \log P - 11.6$. In contrast, an 'urban cold island' effect can be developed in the mornings due to slow warming of urban surfaces as a result of thermal properties of urban materials, tree shade, tall buildings and an increase in albedo associated with elevated pollutant layers. This, however, is somewhat less significant than the urban heat island influence (Ludwig and Kealoha, 1968). Evidence for the prevalence of high daytime urban heat fluxes has also been presented by several field studies. For example, during their study of the St. Louis metropolis, Ching *et al.* (1983) noted that the average mid-day values of heat flux for the month of August were about 120 W/m^2 at a rural site, 135 W/m^2 in a residential area with trees, and 295 W/m^2 at a commercial site devoid of vegetation.

Using a surface meteorological network of 44 stations operated by various public agencies, the monthly-averaged hourly temperature distribution in the Phoenix metropolis could be calculated for January 1998 to delineate the heat island effect. The results are plotted in Figure 6 for 1.00–2.00 AM Note the appearance of an archipelago of urban heat islands within the city. Detailed investigations show that this heat island effect is directly related to urban land use.

Urban roughness effects can appear as large-scale variations in terrain (a few km or more) as well as smaller scale inhomogeneities of built-in elements and trees (tens of meters). These effects are most pronounced under strong background winds ($>$ 3–5 m/s). Buildings cause increased turbulence, resulting in strong vertical mixing and downward momentum transfer in the surface layer, which in turn perturbs the overlying winds. If the buildings are located well apart with little interaction between the wakes of neighboring structures, then the flow around each structure can be treated independently of other elements. This is the 'isolated roughness' regime, which should be contrasted from the 'wake interference regime' where wakes of individual elements interact with one another (Hosker, 1987). When elements are densely packed, stable vortex patterns can be formed in the gaps between the elements, thus forcing the background flow to skim over the top of the roughness array, rather than entering into canyons between the elements and flushing them. According to wind-tunnel studies of Hussain and Lee (1980), for cubical roughness elements of height H arranged in a grid array with face-to-face spacing S, the 'isolated roughness regime' occurs when $S > 2.4H$. The transition of wake interference to the skimming regime occurs when $S < 1.4H$. Nevertheless, it should be noted that the criteria for such transitions can be specific to the dimensions, shape and arrangement of the roughness array (Hosker, 1979; Wilson and Britter, 1982; Rafailidis, 1997, 2001). In addition, when the roughness elements become closer [$< (0.1 - 1)W$], where W is the cross-wind width of the elements, other interesting (and rather paradoxical) flow phenomena can occur (Zdravkovich, 1997). For example, the appearance of bistable, asymmetric, unsteady wakes around the elements that switch between different roughness elements (Goldstein, 1965).

Non-uniformities in roughness make it difficult to generalize flow details from one landscape to another. Examination of previous wind tunnel studies, however, can provide some general qualitative conclusions. With recent increases in the available experimental data, mathematical treatment of non-uniform roughness canopies also has become increasingly feasible; the data can be used to define simplifications necessary for sophisticated analyses (Puttock and Hunt, 1979; Hosker, 1984; Kotaki and Sano, 1981; Belcher and Hunt, 1998). According to Britter and Hunt (1979), the interaction between uneven buildings can be classified as being either strong or weak (cf., the roughness classification given before). Weak interactions occur when one building influences the flow around the next, but itself is not affected by the second building. This situation can be analyzed by simply considering the perturbation to the pressure field. On the other hand, strong interactions are characterized by the influence of downwind buildings on upwind ones, in which case the analysis is intricate and involves vortex dynamics. Most of the studies reported to date on building clusters have been laboratory experiments (Cermak *et al.*, 1974; Penwarden and Wise, 1975; Isyumov and Davenport, 1975; Brechling and Ihlenfeld, 1997). Recent advances in instrumentation (such as the advent of field-scale laser-Doppler anemometers) and the development of test facilities (e.g.,

SLTEST) have enabled high-resolution flow and dispersion studies in the field (Cionco, 1989, 1999).

Previous field and wind tunnel studies demonstrate that: (i) highly intermittent turbulent wakes can be developed between uneven buildings, in contrast to stable and organized vortices that form in canopies of uniform roughness (Isyumov and Davenport, 1975; Baik *et al.*, 2000); (ii) strong pedestrian-level winds can be generated between buildings (Britter and Hunt 1979; McKean, 1984); (iii) smaller buildings can be treated as isolated roughness elements in the regional flow when a city is dominated by a few sparsely scattered, large buildings (Hosker, 1987); and (iv) under certain conditions, the flow around larger buildings can be weakened when smaller buildings are present, whereas local scouring and jetting of fluid around tall buildings can occur under other conditions (Gandemer, 1976; Logan and Barber, 1980). Beranek (1979) has developed rules of thumb to predict various possible flow scenarios in urban building canopies to aid building designs for optimal ventilation, occupant comfort, and pedestrian safety.

As mentioned, the flow and dispersion on intra-urban scales can be highly site dependent. When the incident angle between an urban canyon and the wind direction is large, vortex circulation can be generated within the canyon similar to that between buildings. Conversely, for small incident angles, along-canyon helical circulation patterns can be developed (Johnson *et al.*, 1973). Along-canyon flow cells can also occur when the roughness elements have slanted roofs (Jourmad, 1982; Gong *et al.*, 1996). Traffic-induced turbulence (Qin and Kot, 1993), wind oblique to the street axes (van der Hout *et al.*, 1989) and formation of complex flow patterns at the intersections between canyons are other aspects that contribute to the inhomogeneities of canyon flows. Such spatial inhomogeneities must be properly resolved in street canyon models, if they are to be of practical use, e.g., siting monitoring instruments for regulatory enforcement. According to Dabberdt *et al.* (1973), the carbon monoxide concentration can change by a factor of two to three when an observer crosses the street. It can change by a factor of five when a monitoring instrument is moved from the ground level to a rooftop (Bauman *et al.*, 1982)!

The thickness of the wake layer (Figure 5), in which the effects of roughness elements are felt through non-uniformity of shear stresses, is a quantity of interest in theoretical analysis of urban flows (Jerram *et al.*, 1997). Wind tunnel experiments indicate that the mean velocity and Reynolds stresses are affected up to distances of $\bar{S}$ and $2\bar{S}$, respectively, where $\bar{S}$ is the center to center spacing of the inhomogeneities (Mulhearn and Finnigan, 1978). This differs from the estimates of Raupach and Thom (1981) who found that the roughness sublayer depends on the obstacle heights, their spacing as well as the roof shape. Studies also show that the building influence may extend to about three overall building heights (Rafailidis, 1997; Rafailidis and Schatzmann, 1996) and the upstream and downstream influences of the city on the flow extend to about 20 and 7 street canyon lengths, respectively (Hoydysh *et al.*, 1974).

The central importance of the velocity profile above built-in urban and forest canopies is reflected by the large number of theoretical (Elliot, 1958; Bradley, 1968; Townsend, 1965, 1966; Hunt and Simpson, 1982; Belcher *et al.*, 1990; Jerram *et al.*, 1994, 1997; Belcher and Hunt, 1998), numerical (Wood, 1978; Albini, 1981), physical modeling (Bradley, 1968; Kawatani and Meroney, 1970) and field (Cionco, 1989) studies on this subject. The dynamics of urban and forest canopies have many similarities as well as some dissimilarities, the latter being contributed by the aeroelastic flexibility of trees that leads to their waving in the presence of winds (Finnigan and Mulhearn, 1978). Typically, the approach mean velocity $\bar{U}$ of a roughness canopy close to the ground can be approximated by the logarithmic formula:

$$\frac{\overline{U}}{u_*} = \frac{1}{\kappa} \ln \frac{(z - D_s)}{z_0}, \tag{1}$$

where D_s is the displacement height above the ground, z the vertical coordinate, z_0 the surface roughness, u_* the friction velocity and κ the Karman constant (Arya, 1999). Alternatively, the flow above the ground is usually approximated by a power law form

$$\frac{\overline{U}}{u_*} = \left[\frac{z - D_s}{\delta - D_s}\right]^{\alpha}, \tag{2}$$

where δ is the UBL thickness and α is an exponent (see Uchijima and Wright, 1964).

The perturbations to the approach flow by the roughness canopy have been analyzed using techniques such as the mixing length theory (Cionco, 1965), rapid distortion theory (Belcher *et al.*, 1990), phenomenological models (Albini, 1981) and higher-order turbulence modeling (Wood, 1978). A comprehensive two-dimensional description of the urban boundary layer flow, forced by finite-sized distributed built-in elements, have been reported by Jerram *et al.* (1997) who treated the built-in elements as distributed body forces on the ground. In this model, varying urban effects are captured mathematically by treating the distributed force as a sum of sinusoidal forces with different wavelengths. The problem is solved for each varying wavelength, from which the total solution is constructed. According to their analysis, upon 'feeling' the canopy edge, the flow decelerates over a region proportional to the obstacle height Hwithin a time scale H/U_0, where U_0 is the approach free-stream velocity. Turbulent eddies adjust to the mean perturbations, thus establishing a balance between turbulent stress gradients and the obstacle drag. The removal of momentum leads to an internal boundary layer, whose precise origin is determined by the dynamics of the impact region. At the exit region from the canopy, the flow feels the sudden removal of drag force and accelerates, causing negative velocities sweeping down into the wake.

Regional flows can be perturbed by thermal inhomogeneities on a variety of scales, such as small-scale forcing due to anthropogenic heat sources (e.g., through

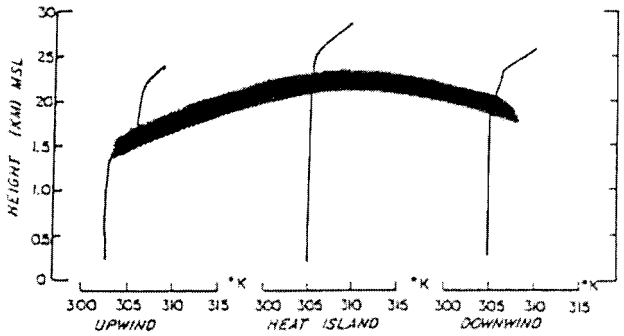

Figure 7. Inversion pattern (shaded) and potential temperature profiles over three sites in St. Louis on July 21, 1975 (from Wong & Dirks 1978).

the tops and sides of buildings, vehicular heat emissions etc.) and inhomogeneities related to urban-scale variation of the energy budget (e.g., urban heat island effect and strong daytime convection in cities). Thermal inhomogeneities modify the boundary layer flow above cities in numerous ways. An example is their influence on the inversion height (Baik and Chun 1997) which, in turn, may affect dispersion and precipitation patterns (Lin and Smith, 1986). The inversion height, z_i, over a city can be as much as 1.5 times that over a rural site (Wong and Dirks, 1978; Figure 7). During nights with rural surface-based inversions, the urban ABL is near neutral up to a few hundred meters, with one or more weaker, thin, elevated inversion layers (Bornstein, 1968; Figure 2). This elevated inversion may be a result of the destruction of stable approach flow by mechanical and/or thermal turbulence. However, the convective character of turbulence, as indicated by stability indices such as w_*/u_*, where $w_* = (q_0 z_i)^{1/3}$ is the convective velocity (Deardorff, 1970), $u_*$the surface friction velocity and q_0 the surface buoyancy flux, does not change appreciably as air enters a city. Both u_* and w_* increase approximately equally except in cases of large roughness change and little heat flux enhancement over the city as would occur in highly vegetated areas. In the laboratory, the urban heat island effect has been simulated by introducing a heat source of finite diameter into a homogeneous or a stratified fluid (e.g., Lu *et al.*, 1997a,b; Figure 8). The direct application of laboratory results to the field, however, is predicated on obtaining compatible surface conditions between the two cases.

The adjustment of flow approaching a city due to changes in thermal forcing is also of interest in urban modeling. According to Briggs (1987), the flow features (both temperature and velocity) tend to equilibrate with the thermal forcing at a downstream distance on the order $(U_0/w_*)z_i$, which is much shorter than that necessary for the adjustment due to roughness inhomogeneities. The thermal inhomogeneities can also have an organizing effect on the flow by generating coherent rolls as evidenced by high temperature/velocity correlation in such rolls. Observations of Kropfli and Kohn (1978) show that these features may be locked on to the surface features, but the mechanism of their generation and reasons for their per-

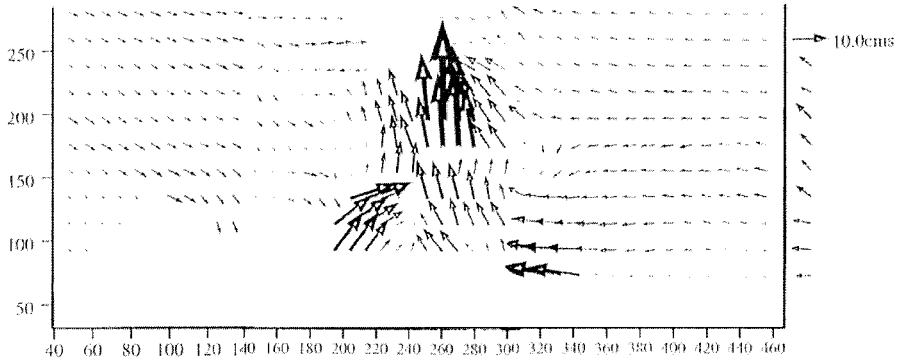

Figure 8. A heat source of finite diameter located at the bottom of a homogeneous fluid; a laboratory experiment mimicking an urban heat island. The velocity vectors of flow above the plume detected by a particle-tracking velocimeter is seen. The experiments were carried out at Arizona State University by the authors.

sistence (both spatially and temporally) are still unclear. Briggs (1987) suggested the use of 'modified' convective scaling $w_*^m = (\Delta q_0 z_i)^{1/3}$ to parameterize such organized structures, where Δq_0 is the incremental heat flux in the warm patch. This proposal awaits detailed experimental confirmation.

As stated earlier, enhanced convective activity above urban heat islands can cause significant perturbations to the regional flow field. Under calm background flow conditions, the thermally induced flow can converge on the urban center and generate a near-surface wind speed maximum at some radial distance from the center (Schreffler, 1978; also see the simulations of Bornstein, 1987). Depending on the lateral extent, the inward flow to the urban center can be affected by the Coriolis force and deflect cyclonically, as observed by Angell *et al.* (1973). Aloft, this layer is a region of diffluence (Ackerman, 1973), where the rising flow is deflected by the overlying stratification. The confluence region can be superimposed on the prevailing flow field and advected downstream (Bornstein and Johnson, 1977; Wong and Dirks, 1978). Observations performed over several cities have shown the existence of a critical speed that divides the low speed, heat-island accelerated flows from the high-speed friction-decelerated flows (Bornstein, 1987), but a criterion to predict this critical speed is yet to be formulated.

Air pollution in cities affects the transfer of solar radiation through the urban atmosphere. The amount of incoming solar radiation can be reduced as much as 20%. Spectral and direction changes occur, since the transmission of shorter wavelengths is more strongly affected. Particles of pollutants also supply nuclei for cloud droplet formation. The average albedo of urban surfaces is lower than that of most soil and vegetation types. This compensates the lower incoming solar radiation in such a way that natural and urban surfaces have similar values of net radiation. The dense material used in urban construction enables a better heat stor-

age. Many urban surfaces are also waterproofed, which increases the water run-off compared to sub-surface water storage.

The modeling of radiative and turbulent energy fluxes over urban terrain is receiving increased attention since it is essential for high-quality modeling of urban wind and temperature fields and hence the dispersion of pollutants. An excellent overview of the problems scientists are facing with respect to the modeling of urban surface fluxes is given in the 'Proceedings of the Third Symposium on the Urban Environment' (2000). With respect to the modeling of surface fluxes, extensive research efforts are under way for defining the roughness lengths and radiative transfer properties of different land use types in urban canopies.

2.2. COMPLEX TERRAIN BOUNDARY LAYERS

The flow in complex terrain can differ greatly from its flat-terrain counterpart, in that a host of new physical phenomena emerge due to topographic influence. A continuum of topographic complexity and scales, synoptic flow, climate, energy budgets and even the scales of the local circulation ensure that generalizations from a particular set or sets of observations are difficult, thus necessitating comprehensive numerical models for predictions of complex terrain flows (Pielke, 1984; Whiteman, 1990). Most of the detailed work in this regard has been on simple isolated topographies, such as hilltops surrounded by flat terrain, rather than on truly complex terrain. These include experimental (Mason and Sykes, 1979; Bradley, 1980; Taylor *et al.*, 1983; Mason and King, 1985; Mickle *et al.*, 1988), theoretical (Jackson and Hunt, 1975; Hunt *et al.*, 1997, 2000), laboratory (Brighton, 1978) and numerical (Hanazaki, 1992) work. Field studies on realistic complex-terrain airsheds have mostly focused on bulk features such as species budgets and mean circulation, and much less on the structure and turbulence (Whiteman and Barr, 1986; Vergeiner and Dreiseitl, 1987; Horst *et al.*, 1987, 1989; Freytag, 1985, 1987; Hennemuth and Kohler, 1984; Hennemuth, 1985, 1986; Kondo *et al.*, 1989; Doran *et al.*, 1990; Maki *et al.*, 1986; Whiteman, 1989; Whiteman *et al.*, 1996).

A physical understanding of flow scenarios in truly complex terrain can be realized by considering simple basic terrain features, such as valleys, slopes, planes and basins. Figure 9(a) shows a valley adjoining a plain and the response of this idealized airshed to diurnal variation of thermal forcing. This is an archetype of many wide-open valleys, such as our home base Phoenix, Arizona (Figure 9(b)). The nighttime flow consists of the drainage of dense air formed on slopes into the valley (down-slope, drainage or katabatic winds) and the channeling of air pooled at the bottom of the valley to the nearby plain (down-valley winds). Drainage winds are driven purely by buoyancy and are separated from the ambient fluid by a strong shear layer at its outer edge, which evolves into instabilities and turbulence (Ellison and Turner, 1959; Simpson, 1997). During the daytime, the flow is up-slope (anabatic winds) and is compensated by subsidence of warm air into the valley. These flow phenomena compounded with topographic amplification (higher temperatures

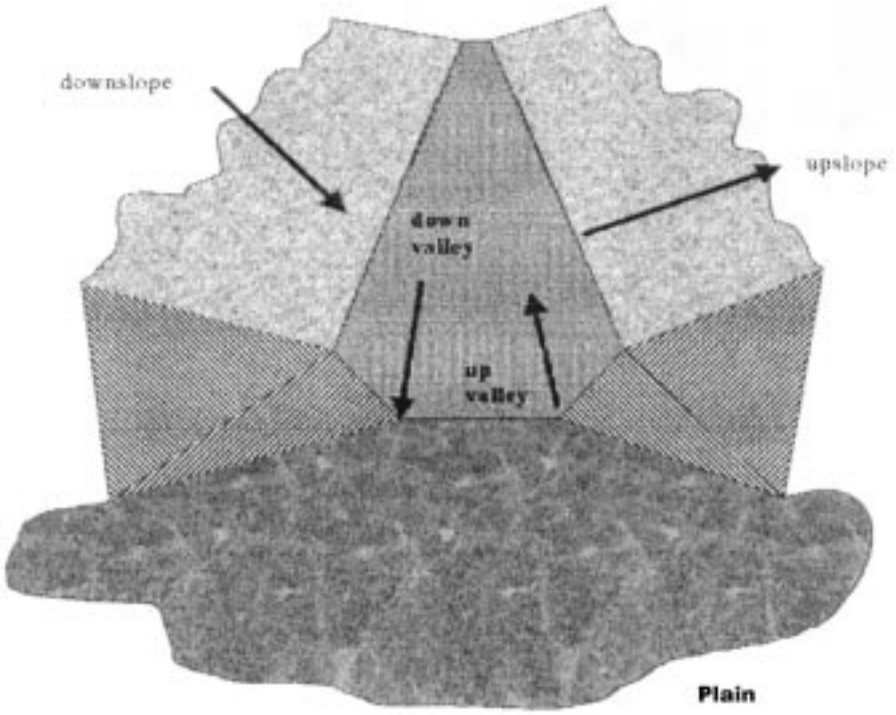

Figure 9a. An idealized valley adjoining a plain showing the up and down slope winds and up and down valley winds. (b) The complex terrain surrounding Phoenix, Arizona. Some key cities, sites of PAFEX field experiments (Section 4), and the Phoenix Sky Harbor International Airport are indicated. Scales of katabatic winds induced by adjacent slopes (10 km) and drainage flow through the complex topography (100 km) are indicated.

in the valley than on the plain due to lesser amount of air contained below a given ridge-level plan area; Whiteman 1990) lead to a down-valley hydrostatic pressure gradient and hence to an up-valley flow. If the city is located close to the ocean (e.g., Los Angeles) or large lakes (Salt Lake City), additional complications are possible due to lake and sea breeze (Lu and Turco, 1994).

In basins (i.e., low-lying areas where the air movement is constrained by surrounding topographic features; Figure 10), the along-valley flows are either weakened or completely eliminated, leading to significant pooling. At night, katabatic flows originating at different levels on the slope are subjected to entrainment and mixing with the background fluid, creating air masses of varying densities that sliver into the cold pool in the form of intrusions propagating at their equilibrium density levels. Since flows of different densities originating at slopes of varying orientation contribute to pooling, the flow therein can be construed as a vertically skewed stratified shear flow (Figure 11), with predominantly horizontal intrusive motions amenable to instabilities and turbulence. Since katabatic flows in a basin are confined to a narrow density range and since small-scale vertical mixing is

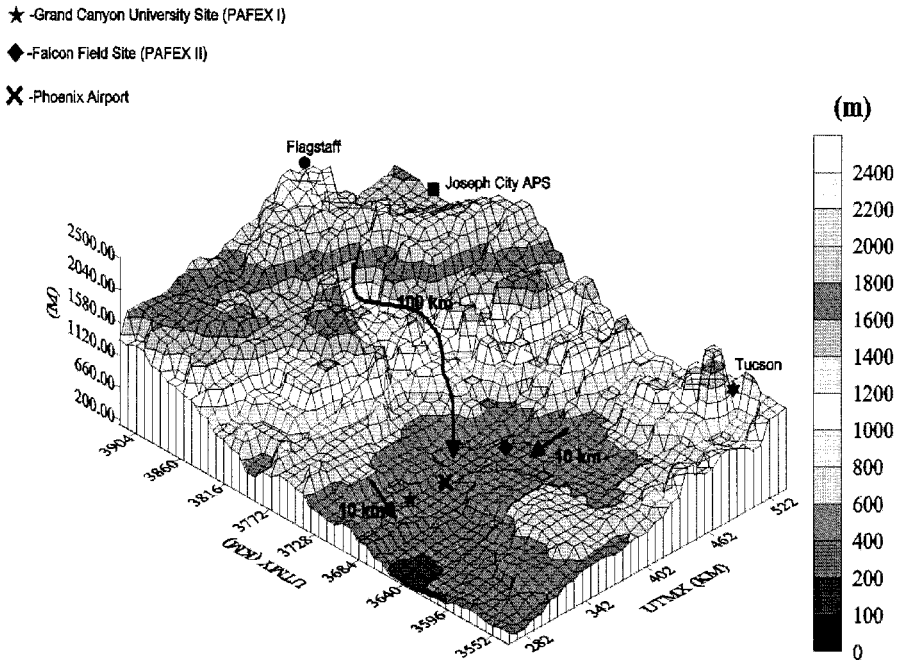

Figure 9b. The complex terrain surrounding Phoenix, Arizona. Some key cities, sites of PAFEX field experiments (Section 4), and the Phoenix Sky Harbor International Airport are indicated. Scales of katabatic winds induced by adjacent slopes (10 km) and drainage flow through the complex topography (100 km) are indicated.

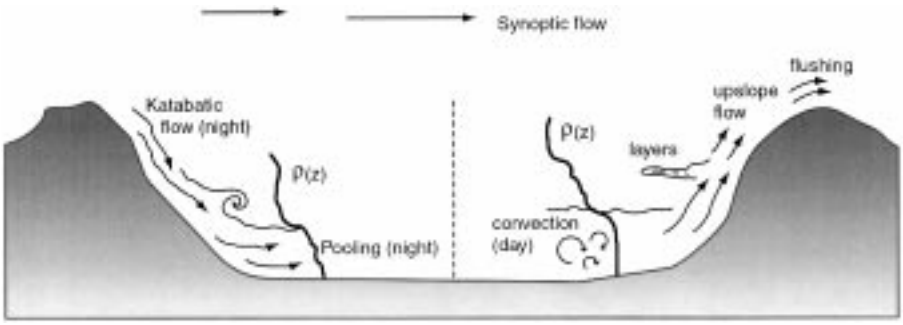

Figure 10. A schematic of a complex terrain basin.

possible between different density layers, the vertical density gradient (and hence N) in a cold pool can be significantly lower than that of a flat-terrain SBL. Ensuing low Ri_g values can facilitate sustained turbulence within the pool *vis-à-vis* the intermittent turbulence in flat-terrain SBL. A significant buoyancy jump (an inversion), however, can exist at the top of the cold pool, which may act as a barrier to vertical mixing. The shear turbulence, therefore, is expected to smoothen the density profile *via* vertical mixing, but does not contain eddies that can overturn the cold pool. At times, cold air can overflow out of the basin into surrounding

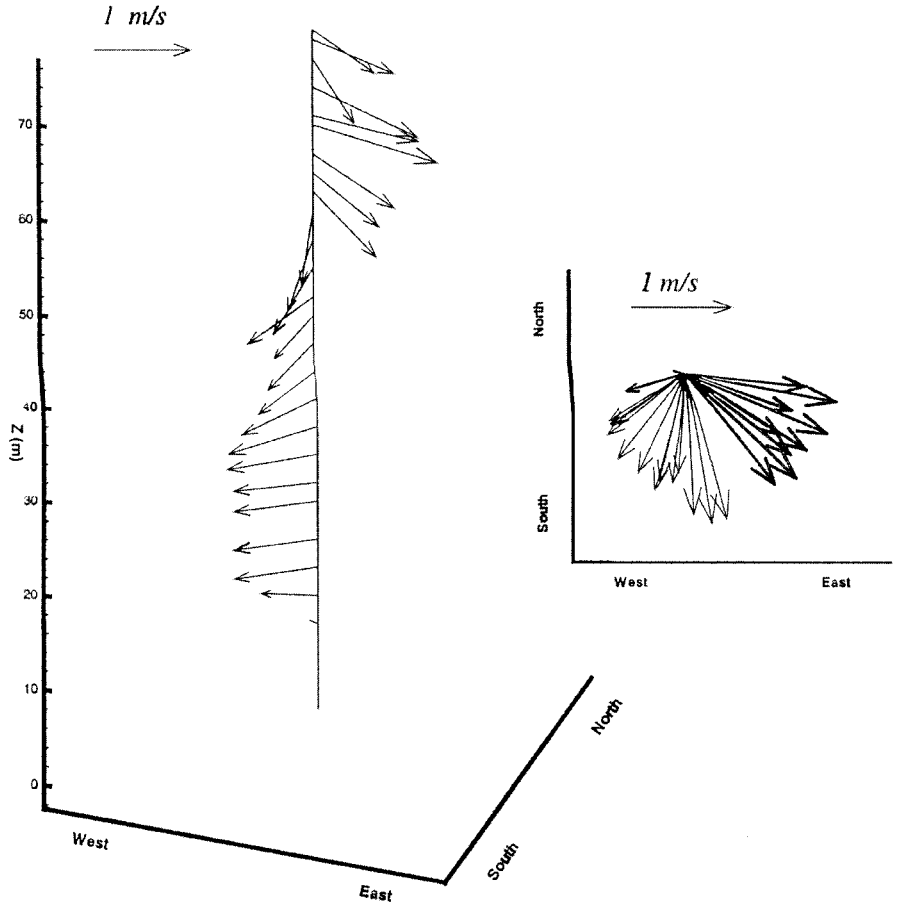

Figure 11. A skewed stratified shear flow measured in the Central Phoenix Valley at Grand Canyon University ground (Figure 9(b)) on January 22, 1998, 6:24 to 6:27 A.M. Different air masses intrude into the basin at different heights. A tethered balloon was used for measurements (Section 4).

areas, leaving a weakly or moderately stratified pool capped by an inversion, above which the stratification is neutral. Pooling is also possible in valleys with restricted entry and exit conditions. In this case, the extent of pooling depends on a number of factors, including topographic barriers, valley geometry and hydraulic control at the valley mouth. For example, short valleys tend to empty pooled air onto the plane more rapidly. At night, stable stratification is a common feature in valleys.

Figures 12 and 13 show a laboratory experiment in which a two-dimensional basin is subjected to bottom heating and cooling. The basin was designed to represent the two-dimensional numerical model of Kuwagata and Kimura (1997), in which the shape of the Ina valley in Japan (40 km wide, 2–2.5 km deep) was approximated by a sinusoidal basin. As in the numerical model, the temperature (heat flux) of the basin floor was varied sinusoidally. This is achieved by pumping water

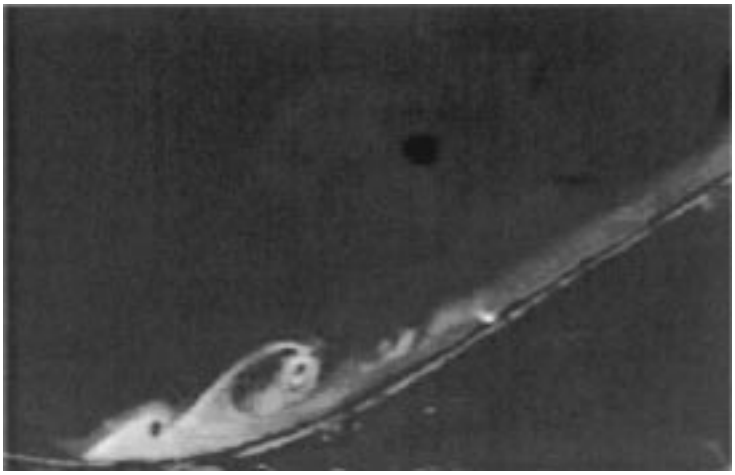

Figure 12. Laboratory experiment designed to simulate katabatic flow in a basin. Note the down-slope flow into the basin. The shear between the katabatic flow and the turbulent fluid generates overturning instabilities. The laboratory experiments shown in Figures 12 and 13 were carried out at Arizona Sate University.

of controlled temperature to a cavity beneath the basin, wherein the thin copper sheet metal floor allows the temperature changes in the cavity to be instantaneously transmitted to the fluid. As before, the working fluid of the model is water, and turbulent flow conditions in the tank can be obtained by maintaining high heating/cooling fluxes (peak ~ 1000 W/m^2). The model was instrumented with a rake of thermocouples, a particle-tracking velocimeter and a laser-induced fluorescence system, permitting detailed investigations of basin boundary layers. Initial testing of the apparatus showed promising qualitative results, in that it reproduced pooling and the breakup of the inversion satisfactorily. Note the development of pooling flow, in the form of katabatic flow over the slopes and the development of Kelvin–Helmholtz billows at the top of the slope flow. The use of such process-oriented laboratory experiments and associated theoretical analyses to elicit flow processes occurring in urban areas is expected to be a key component of UFM.

In the early morning, heating of the ground generates a shallow, neutral CBL at the bottom of the basin, much the same as over flat terrain (Figures 10; 13(a) and 13(b). Concurrently, a weak up-slope mean flow is developed within a thin boundary layer, transporting heated valley air past the inversion. Lateral mixing of this up-slope flow with the background air generates air parcels of varying densities. When the basin is stably stratified (e.g., in the morning), fluid elements from the up-slope flow can intrude into the warm stable core at their neutral buoyancy level, disturbing the stratification (i.e., producing a variable lapse rate) and possibly forming a layered structure as shown in Figure 13(b). By mid day, with the intensification of heating, the up-slope flow strengthens, removing substantial amounts of turbulent air from the CBL and creating a compensatory subsidence in

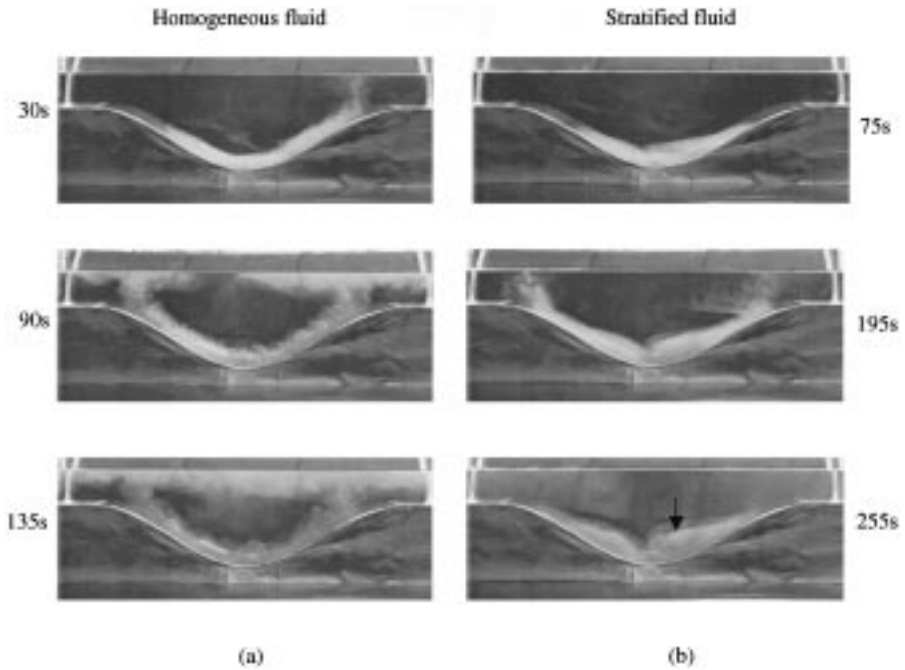

Figure 13. The development of upslope flow in a laboratory basin subjected to bottom heating. Dye has been used for flow visualization: (a) homogeneous background fluid and (b) linear stratified environments. Note the rise of flow along the boundaries and its separation near the rim of the basin. In the homogeneous case, the separated flow rises to the top of the fluid layer and spreads horizontally. The fluid core above the basin descends with time and entrains into the rising flow. Therefore, some of the contaminants released near the ground may later reappear via the subsidence flow. In the stratified case, the upslope flow intrudes back into the basin (see the arrow) and re-entrains into the convective layer. The flow separation at the rim is weak in this case. The times after the initiation of heating is given. The laboratory heat flux corresponds approximately to 1000 W/m^2 in nature.

the middle of the basin (Davidson and Rao, 1963). The competition between the subsidence of the stable core and the growth of the CBL determines the daytime flow and transport in the basin.

The interaction of the cold pool with a travelling synoptic weather system is also of interest (Doran, 1991). The velocity shear, ΔU, between the winds aloft and the cold pool can exert a destabilizing influence on the interface between the two layers. If the buoyancy jump across the interface is Δb, then the interfacial response is expected to be governed by either Ri_g or the bulk Richardson number $Ri = \Delta bL/(\Delta U)^2$, where L is the characteristic lengthscale of the upper flow (Fernando, 1991; De Silva *et al.*, 1999). At low Ri_g, shear instabilities such as Kelvin–Helmholtz billowing (Strang and Fernando, 2000) can be generated, the breakdown of which may generate intense turbulence that scours and erodes the cold pool, eventually breaking it up completely. If the cold pool sustains sufficiently high levels of turbulence, then the above *Ri*-based criterion should be modified to

account for differential turbulence forcing on the interface (Fernando, 1995). The shear-driven cold pool break-up phenomenon has not been subjected to systematic study, although the flushing of small dense pools has received some attention (Briggs *et al.*, 1990; Castro *et al.*, 1993; Debbler and Armfield, 1997).

3. Urban Air Quality Issues

Major urban areas, regardless of geographic setting, tend to be centers of high concentrations of numerous air pollutants. The most widespread and pervasive of these pollutants are included in the USEPA's six 'criteria air pollutants': ozone (O_3), carbon monoxide (CO), nitrogen dioxide (NO_2), PM_{10} (particulate matter smaller than 10 μm in diameter), lead (Pb), and sulfur dioxide (SO_2). The spatial and temporal variations in their concentrations result from a fully coupled system of chemical and meteorological processes. In areas of complex terrain, the surface concentrations of these pollutants are strongly influenced by trapping within basin topography and the thermally driven transports that operate within the basins. Other related influences are the presence or absence of stable stratification and instabilities that cause mixing between layers in the lower troposphere.

Relative to the time scale of local atmospheric transports, two categories might be considered for pollutants in urban complex terrain: inert and reactive. Some criteria pollutants are essentially inert and are determined by advection, dispersion, and deposition. By mass, most PM_{10} is included in the inert category. Secondary aerosols, those formed by gas to particle conversion, are not strictly inert but are rarely dominant in terms of aerosol mass. Aerosol Pb is essentially inert, although the form of the lead may change in the ABL, and CO is for practical purposes inert on the time scale of a day or so. The remaining three criteria pollutants, O_3, NO_2, and SO_2, are typically involved in chemical reactions that are rapid on the ABL time scale. Their concentrations, therefore, are influenced not only by their transport but also by the transport of reactants in the chemical processes that form or destroy them. For instance, if different necessary reactants are prevented from mixing by the transport processes, then important reactions can be inhibited; an example would be precursors of O_3 separated from NO_x (NO and NO_2) formed later in the day in the same source location.

In the U.S., the Clean Air Act as last amended in 1990 requires the U.S. Environmental Protection Agency (USEPA) to establish National Ambient Air Quality Standards (NAAQS) for the criteria air pollutants. There are both primary standards, based on public health effects including on sensitive segments of the population, and secondary standards, based on effects on public welfare such as visibility and economic impact on agriculture (USEPA 1997). The trend over time has been toward uniformity in the primary and secondary standards. We consider here the three criteria pollutants for which the standards are most often exceeded in U.S. urban areas in complex terrain: O_3, CO and PM_{10}. The introduction of catalytic converters in automobiles and trucks has greatly reduced the levels of NO_2 pol-

lution, although it remains a key species in the formation and destruction of O_3. With the discontinuation of leaded gasoline and the closure of many non-ferrous smelters, Pb is no longer as serious an air pollutant as it once was. However, there are still point sources for aerosol Pb in some locales. SO_2 tends to be a problem only in areas with smelters or coal-fired power plants. In the Southwest U.S., most of the SO_2 sources are in rural areas, although meso-scale flow can transport SO_2 or its aerosol reaction products into urban areas.

The current NAAQS for O_3 is a 1-hour average of 120 ppb. An 8-hour standard of 80 ppb was introduced in 1997 but blocked by court action. Because O_3 is formed and destroyed by rapid chemical reactions involving volatile organic compounds (VOCs), NO_x (i.e., NO and NO_2), CO, and other gaseous species, the transport and mixing of both ozone and reactants (and reservoir species for the reactants) must be considered. NO_x is essential for both the formation and destruction of O_3, and it comes from combustion sources; automobiles are the most important source in many urban areas but industry can also be important. VOCs are largely from automobiles as well, especially from uncombusted fuel that was either spilled or not completely burned because of poor engine tuning. In some areas, industrial sources of VOCs can be important, as can be natural emissions from vegetation. When VOCs and NO_x react with oxygen in the presence of strong sunlight and heat, ozone is formed and under some conditions their concentrations can rise to unhealthy levels. This ground-level ozone should not be confused with ozone that forms high in the stratosphere and shields Earth from the Sun's harmful ultraviolet rays.

Carbon monoxide is formed by the incomplete combustion of fossil fuels, either by motor vehicles or industry. Automobiles tend to be the dominant urban source. The NAAQS for CO is currently 35 ppm for a 1-hour average and 9 ppm for an 8-hour average. In urban areas of the Southwest U.S., the highest concentrations occur during the winter months when stable inversions develop and persist. In the summer months, with higher temperatures and solar radation flux, CO can participate in O_3-forming photochemical reactions. However, even in summer, its lifetime is much longer than that of VOCs and can be considered relatively inert.

The NAAQS for PM_{10} is 150 μg/m^3 averaged over 24 hours. There is also an annual mean standard of 50 μg/m^3. Unlike the other criteria pollutants that have known toxicity, PM_{10} lumps together the mass of all particle types, whether toxic or benign. Responding to substantial evidence that respiration of high concentrations of fine particles, those smaller than 2.5 μm in diameter, impacted public health the USEPA tried in 1997 to introduce a $PM_{2.5}$standard of a 24-hour average of 65 μg/m^3. This new standard was also blocked by court action.

4. Flow and Air Quality in Urban Valleys: Case Studies

Air quality in urban valleys is largely determined by the way background synoptic winds interact with local thermal (slope/valley) circulation. Strong synoptic

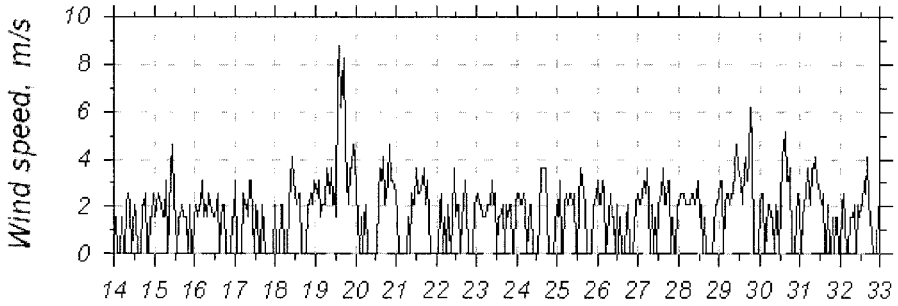

Figure 14. The wind speed measured at the Phoenix Sky Harbor International Airport during the month of January 1998. Note the recurrence of diurnal flow changes except for several days where strong synoptic flow was present.

winds can penetrate and flush pollutants from urban basins, thus overshadowing the confining effects of the terrain (Mahrt, 1990; Whiteman and Doran, 1993). Many complex-terrain cities, particularly those in the 'Sun Belt' of the Southwestern U.S. (e.g., Phoenix, El Paso and Las Vegas), nevertheless, are located in areas characterized by high pressure and low synoptic winds (Wang and Angell, 1999), and their microclimate is dominated by local thermal circulation. Low surface winds, impact of pollutants on terrain, accumulation of flow (and pollutants) in the valleys due to restricted entry and exit conditions and the drainage of katabatic flow to population centers are characteristics of these areas (Dickerson and Gudiksen, 1984; Hanna and Strimaitis, 1990; Richards *et al.*, 1991; Allwine, 1992; Cionco *et al.*, 1999). The resulting pollution build up has plagued a number of U.S. cities, including Phoenix, Arizona which has been classified by the USEPA as 'serious' for non-attainment of NAAQS for O_3, PM and CO. Approximately 70% of the year, the synoptic flow in this area is weak and local slope and valley winds are dominant. Figure 14 shows the nature of diurnal flow in the Phoenix area, which is nominally recurring in the winter due to the absence of synoptic flow. The resident times of air masses within the basin are long, thus providing conditions conducive for the pollution build up in the city. Los Angeles is another area where the complex terrain contributes to the pollution built up. In this case, the local circulation is modified by the presence of sea breeze which drives the diurnal flow inland and seaward (Lu and Turco, 1994).

Two field experiments, known as Phoenix AirFlow Experiments (dubbed PAFEX-I and PAFEX-II), were conducted during the winter and summer of 1998 to study the flow and air quality in Phoenix valley. Both were major meteorological and air quality studies, with applicability to diverse scientific interests. PAFEX–I was carried out at Grand Canyon University premises (January 14–February 4, 1998), which is located in a 'hot spot' for PM and about one mile north of a winter 'hot spot' of CO (Figure 9(b)). PAFEX-II was conducted at the Falcon Field Municipal Airport (July 15–September 15, 1998), sited in the path through

Figure 15a. A photograph showing the PAFEX-I instrumentation. It consists of a tethered meteorological tower carrying the sondes and a ground meteorological station. (b) A 'streaker' suspended from the meteorological tower.

which ozone and its chemical precursors originating in the central Phoenix area are transported northeastward in the summer.

During PAFEX-I, the vertical distributions of wind velocity, temperature and relative humidity were measured using a tethered meteorological tower. A portable surface meteorological station recorded the data of the near-surface temperature, humidity, pressure, wind speed and wind direction, and solar radiation (Figure 15(a)). A unique feature of the experiment was the sampling and subsequent chemical analysis of both fine and coarse aerosols; filter sampling based on 'streaker' instruments attached to the tether wire was used for this purpose (Figure 15(b)). For PAFEX-I, a programmable streaker sampler was modified so that it could be attached to the tether of the meteorological balloon. Samples were collected at ele-

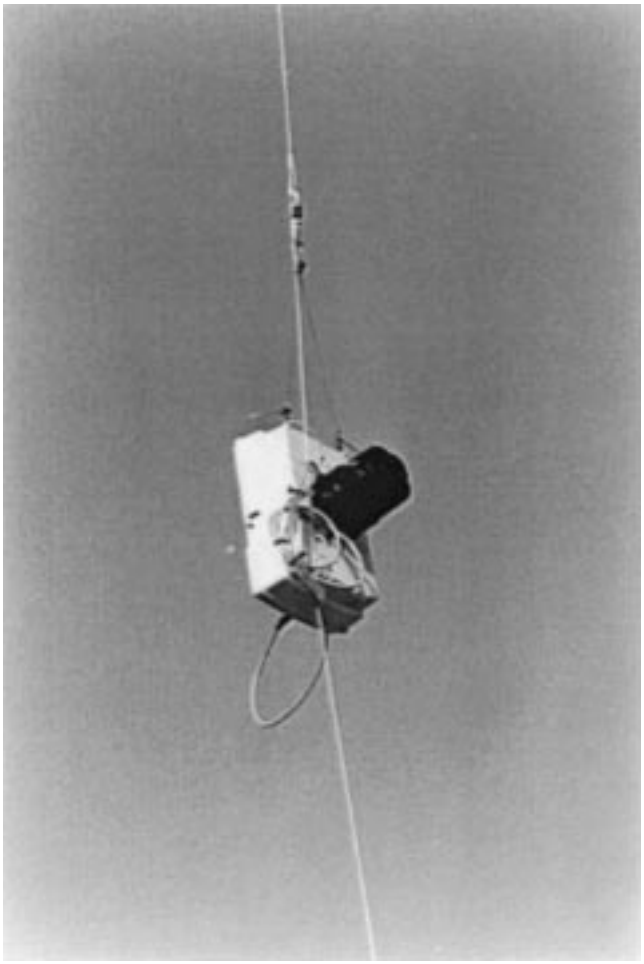

Figure 15b. A 'streaker' suspended from the meteorological tower.

vations from ground level up to 300 m over short time periods (11–15 min) in order to investigate the variation of particle concentrations and size distributions with time and altitude. Such particles act as excellent 'tracers' to determine the sources and trajectories of pollutants. In addition, the criteria pollutant concentrations were measured during PAFEX-II, which established databases of O_3, PM, NO_x and NO_y (other nitrogen oxides) and meteorological variables, enabling investigations into the characterization of chemicals and their transport and mixing by the flow. In both experiments, turbulence data were obtained at 10m above the surface with a fast-response sonic anemometer that measured all three components of the wind vector and temperature. Concurrently, data were gathered from forty-four routine monitoring stations in the Phoenix Valley, which included the sites operated by the Arizona Department of Environmental Quality (ADEQ), Phoenix Real-time Instrumentation for Surface Meteorology Studies (PRISMS), Sky Harbor International

Airport, the Flood Control District of Maricopa County (ALERT), the National Weather Service (NWS), and the Arizona Meteorological Network (AZMET) of the University of Arizona. In addition, several numerical forecasting models were used to predict the flow (MM5 and HOTMAC models), dispersion (RAPTAD, CAL3QHC) and pollutants (Models-3) during the experimental period, and the predictions were compared with measurements (Section 5).

The measurements revealed how, during the middle of the day, the pollutant-laden warm air moves up the valley and up the slopes towards the surrounding mountains, whence the convective boundary layer thickens up to heights of well over 2 km in the summer and 0.75 km in the winter. The pollutants are mixed to this height and usually move northeastward through the valley. In the late afternoon, with subsiding solar radiation and cooling of the ground, mixing decreases and a stable layer of air develops near the ground. Toward the night, the flow is typified by the down slope (katabatic) and down valley winds that originate either on slopes surrounding the valley (10 km scale) or on the large-scale terrain to the north (100 km scale). Gravity current fronts associated with the 10 km-scale flow reach the valley early in the night ($\sim$ 7 PM) whereas the fronts of the meso-scale flows arrive early in the morning ($\sim$ 1 AM).

Figure 16 shows the aerosol samples collected at various elevations from ground level up to 300 m with sampling time of 11 to 15 min. Particles were analyzed using an automated Scanning Electron Microscope, which allows determination of the chemical composition and size of a representative particle population, based on the individual particle analysis methodology described by Anderson *et al.* (1996). This method allows the determination of the chemical composition, size, and shape of individual inorganic particles within the size range of 0.1 μm to 10 μm, covering the inorganic fractions of $PM_{2.5}$ and PM_{10}. The particles can then be divided into chemically distinct particle types, and the concentrations and size distributions of each type can be determined. A number of particle types could be identified in PAFEX-I, differentiated by chemical composition of the aerosol (Figure 16(b–d)). One anthropogenic type, sub-micron spheres of iron oxide, was useful as an aerosol marker to help in integrating aerosol data with the modeling efforts.

The typical velocity structure that prevailed during the measurements is shown in Figure 17, indicating the presence of a well-defined low-level jet of which the wind speed is about 8 times that at the surface (also see Fast *et al.*, 2000). The particle concentration displayed a maximum at the height of the jet, indicating the possibility of jet carrying particles from elsewhere. The important particle types include mineral soil and soot, and the calculated back trajectory indicates the air-mass has passed over an area in the urban core some three miles away where two major freeways intersect. This elevated ($\sim$30 m) jet is the major mechanism for aerosol pollutant transport, but the surface concentrations are not strongly affected by this transport until vertical convective mixing occurs. During the measurement period, however, the lower atmospheric mixed layer evolved, precluding detailed investigations on how the aerosols transfer from the jet to ground level. Better space

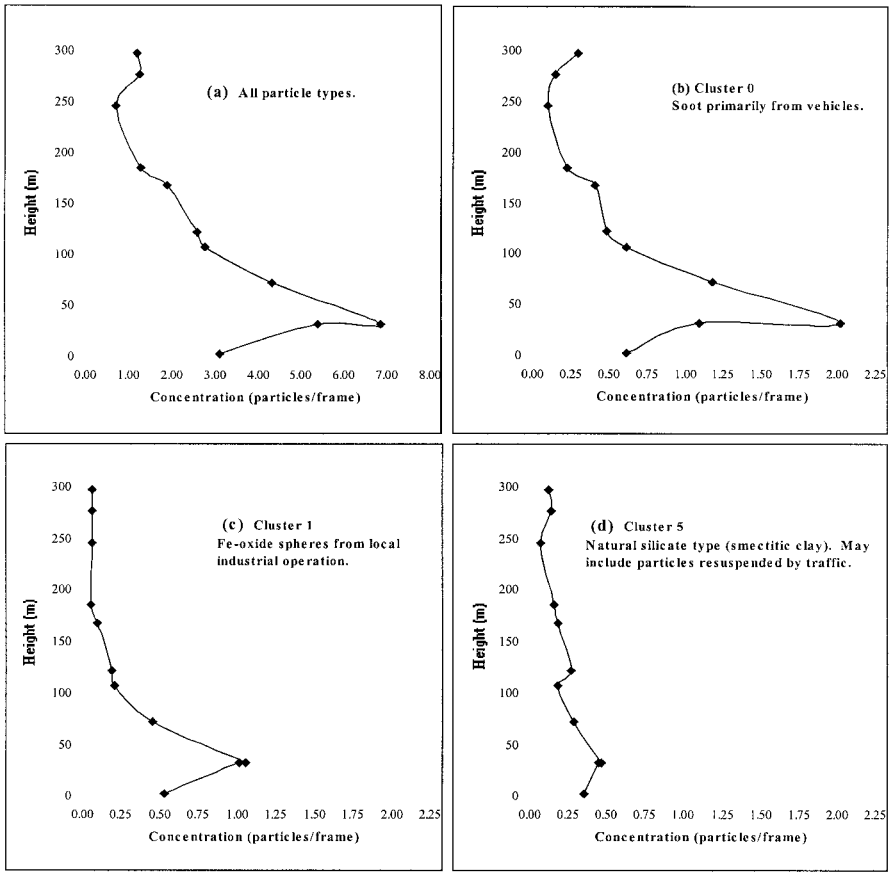

Figure 16. Aerosol particle data for January 23, 1998, 8:30 to 10:30 A.M., taken during PAFEX-I. Concentrations versus height profiles for (a) total particles and (b)-(d) three chemically distinct particle types.

and time resolved aerosol data can yield useful information on such mixing, and obtaining such data will be a major task in future studies.

During PAFEX-II, a different sampling strategy was used to investigate the transport of the Phoenix pollution plume up the valley. Here, the aerosols were sampled at 5 m next to the inlets for instruments measuring ozone, NO_x and NO_y, using sampling times of one to two hours. During the summer ozone season, daytime valley and slope flows can drive a plume of O_3 precursors from the source area in the urban core to outlying areas (east valley) remote from significant sources as much as 50 km (Heisler *et al.*, 1997) (Figure 18). One important result of such a process is the removal of photochemically produced O_3 from NO_x formed later in the day in the urban core; this can reduce the extent of O_3 destruction by reacting with NO_3 radical in the night. Reverse nighttime terrain flows can also return remaining O_3 to the vicinity of the original source area, thus increasing the concentrations on

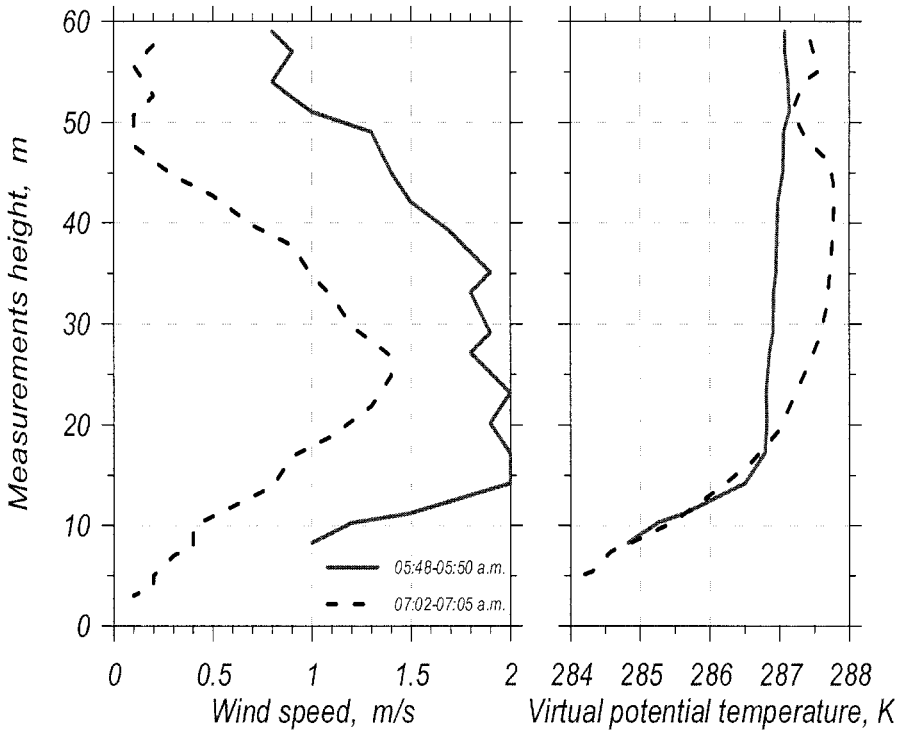

Figure 17. Velocity and virtual potential temperature profiles through the jet observed at 5:48 to 5:50 A.M. and 7:02 to 7:05 A.M. January 22, 1998.

the following day if favorable meteorological conditions persist. Ellis *et al.* (1999, 2000) describe the climatology of ozone plume formation during PAFEX-II. The relative timing of the particle front and the ozone peak vary considerably from day to day, presenting a set of challenging problems to relate the pollutants to the background flow and turbulence (Figure 18).

A similar study dealing with ozone plume transport has been conducted in the urban air basin of Madrid, Spain (Plaza *et al.*, 1997). Madrid lies in complex terrain and is similar to Phoenix with regard to ozone except that slope flows are more dominant in transporting the plumes. When the influence of the Azores High extends over the Iberian Peninsula, high temperatures, low meso-scale wind speeds and clear-sky conditions prevail, the same general conditions that prevail when a stable high-pressure system sits over Phoenix. A diurnal cycle of slope heating and cooling of the Guadarrama mountain range acts as the main driving force of air circulation in the Madrid basin. As in Phoenix, the transitions from heating to cooling and cooling to heating are periods of very low wind speed and are followed by a reversal in flow direction whenever the synoptic conditions allow local circulation to develop. In Madrid the ozone plume is confined to a mixed layer extending from the surface up to an inversion which at noon is 1000 to 2000 m

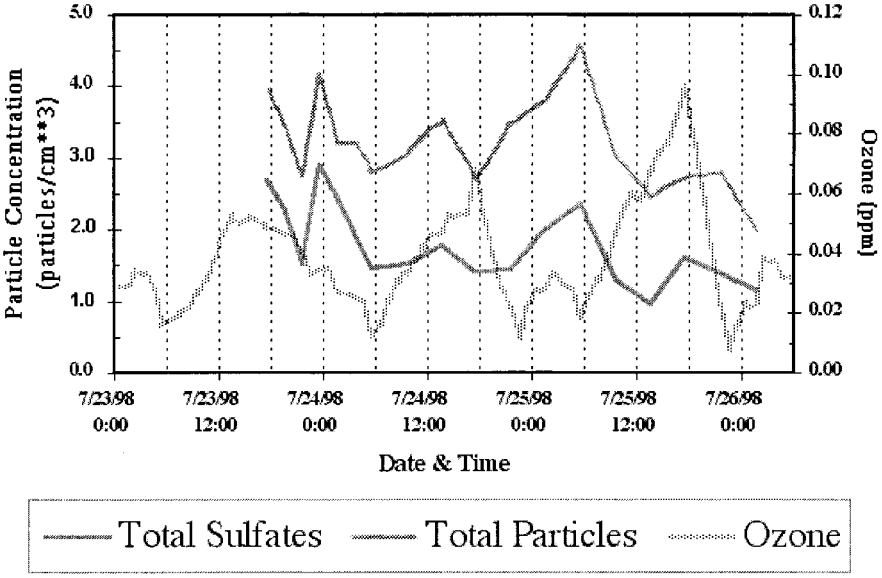

Figure 18. Measurement of surface-level total sulfates, particles, and ozone during PAFEX-II. Evidence for the arrival of an ozone plume in the late afternoon/evening can be seen. The ozone precursors emitted by motor vehicles in the valley are transported by the up-valley flow at a speed 1–2 m/s and arrive in the measurement location in the evening (1800 hrs). During transit, the ozone precursors are 'baked' and the ozone formation process is completed in the evening approximately when the plume arrives at the ozone hotspot where PAFEX II was conducted. The concentration of particles does not follow the ozone, implying that the particles are arriving from sources other than traffic in the valley. The sulfates, however, follow the concentration of particles, implying that they are from similar sources.

AGL and which deepens by convection to 2000 to 3000 m in the afternoon. In the early morning hours, the radiative inversion can still be found at up to 300 m AGL although about one hour after dawn it is entirely destroyed. The Madrid ozone plume advects a distance of 50 to 100 km daily and has maximum measured hourly values of 140 ppb, commensurate with the results obtained in the Phoenix studies.

Further examples of long-range transport of aerosols aloft, followed by mixing down to the surface (which is known as *fumigation*) were found during the Paso del Norte Air Research Program (PDNARP) in El Paso, Texas. Sodium sulfate particles with minor element concentrations indicative of sea salt that has reacted with sulfate were found periodically during a brief study during December 1998. In these studies 2-hour samples were taken from an inlet 5 m above ground and analyzed by automated scanning electron microscopy. The nearest source of sea salt is the Gulf of Mexico, several hundred kilometers away. Coal combustion aerosols dominated by ammonium sulfate were also observed, but in association with soot and spherical fly ash particles. Coal is not used in the El Paso–Cuidad Juarez urban area, but a number of power plants and smelters to the south and southeast use coal. From the beginning until midday on December 3, the synoptic

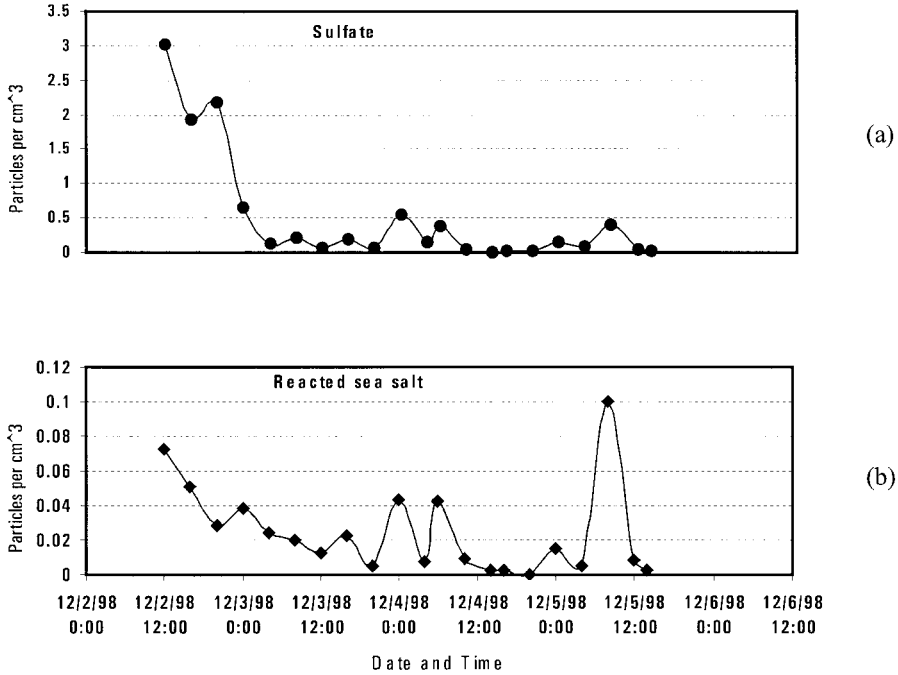

Figure 19. Number concentrations of sulfate and reacted sea salt from the Sun Metro sampling site during 1998 PDNARP field campaign. Samples were two hours in duration. Dry particle diameters were in the range of 0.15–10 microns. Single-particle analyses were performed using automated scanning electron microscopy.

winds from the south were dominant and both reacted sea salt (Figure 19(a)) and sulfate particles (Figure 19(b)) were in relatively high concentration. Later in the period, synoptic winds were no longer dominant and circulation transported local pollutants. However, there were several brief events during which several aerosol types from distant sources were observed, including an event during the evening of December 5. It is suspected that this is due to a vertical mixing event that brought upper-air aerosol to ground level. Vertical profiles of wind and potential temperature, however, were not measured simultaneously and hence the nature of the instability that led to such mixing could not be ascertained.

5. Modeling of Urban Flows

Meteorological flow fields of urban scales are in the realm of meso and micro scales, and they can be calculated using either diagnostic or prognostic techniques. The diagnostic approach is essentially an interpolation method based on measurements subject to proper physical constraints (e.g., conservation of mass, momentum, and vorticity). The variational method (Sasaki, 1970) has been one of the most popular diagnostic techniques (Sherman, 1978; Dickerson, 1978) and in the

regulatory context, the USEPA's Diagnostic Wind Model (DWM) has been widely adapted for generating micrometeorological flow fields (Berman *et al.*, 1995). Kaplan and Dinar (1996) have used diagnostic techniques to obtain much finer scale distribution of winds in the displacement, cavity and wake zones around a building. In prognostic methods, the temporal and spatial distributions of meteorological variables are generated *via* solving primitive equations numerically, and they are much more computer intensive. Prognostic models are broadly classified into hydrostatic incompressible (hydrostatic versions of MM5 version 2 (Grell *et al.* 1994) and HOTMAC (Yamada, 1981)) and nonhydrostatic compressible (MM5 version 3 (Dudhia *et al.*, 2000); RAMS (Pielke *et al.*, 1992); ARPS (Xue *et al.*, 1995)) types, the latter requiring extensive computer resources. Over the last few years nonhydrostatic models have been popular in urban scale applications, keeping pace with the progress of computer hardware technology. Theoretically, nonhydrostatic models are the most appropriate for urban predictions, since urban computational domains do not satisfy the requirement of very small aspects ratio (height/width) necessary to justify the hydrostatic assumption.

Several constraints limit the direct application of meso-scale models for urban flows. First, the terrain-following coordinate system used in meteorological models is not applicable for cases of flow around buildings. This is because slopes of 45 deg or less are required by the hydrostatic assumption (Pielke, 1984) and numerical stability also requires shallow slope angle of terrain. In addition, 90 deg slopes cannot be represented with the gridded system of terrain-following coordinates. Typical examples of terrain following coordinates are the sigma coordinate of MM5 (Grell *et al.*, 1994) and the z^* coordinate of RAMS (Pielke *et al.*, 1992), ARPS (Xue *et al.*, 1995) and HOTMAC (Yamada, 1981). Secondly, the morphology of land use features is not properly implemented in current mesoscale models. Only one 'urban' category exists in the land use classification for mesoscale modeling, although there are significant differences of roughness length, albedo, emission of anthropogenic heat, etc. between residential areas and commercial areas with skyscrapers within the same 'urban' category. Worse still, not a single urban category is employed in some models. For example, ARPS does not contain an urban category in its classification of soil and vegetation (Xue *et al.*, 1995) nor does one of the MM5's land use classifications (i.e. the 17-category SiB vegetation classification; Dudhia *et al.*, 2000). Thirdly, resolving well-known urban phenomena, for example urban heat islands and momentum drag due to a cluster of buildings in mesoscale models, remains a bane of urban modeling. Uno *et al.* (1989), Urano *et al.* (1999), and Yamada (2000) have developed schemes to represent such phenomena within the frame of mesoscale modeling.

While a mesoscale model needs to be 'scaled-down' to simulate urban wind flow, computational fluid dynamics (CFD) models can be 'scaled-up' for the same purpose. CFD is being widely utilized in engineering flow analysis and building and structural design applications, and its utility for urban wind flow predictions has been increasingly recognized in recent years (Baik and Kim, 1999). CFD has

been used not only for urban flow simulations, but also for estimating air pollutant concentrations and human exposure (Cheatham *et al.*, 2000; Emery *et al.*, 2000; Chan *et al.*, 2000, Huber *et al.*, 2000). In the urban flow modeling community, however, CFD is often viewed with caution as an advanced, numerically expensive computational tool with questionable utility in simulating meteorological processes that are largely statistical rather than deterministic in character (Lee *et al.*, 2000). In addition, specification of accurate boundary conditions required for CFD is not tenable in urban modeling. Recently, meso-scale and CFD models have been jointly used to perform simulations of urban wind flow in a nested configuration (Smith *et al.*, 2000; Cox *et al.*, 2000). Brown *et al.* (2000) describe multi-scale nested modeling that incorporates the meso-scale model COAMPS (Coupled Ocean/Atmosphere Mesoscale Prediction System), the multiple building scale model HIGRAD (High Gradient) model, and the single building scale CFD model FEM3MP (Finite Element Model 3). One of the promising ways of simulating urban flows is to nest a meso-scale model that generates a mean state of meteorological variables with a CFD model dealing with perturbations to the meso-scale flow by variability within urban morphology.

5.1. SIMULATION OF AIR FLOW IN THE PHOENIX METROPOLIS

The flow fields during PAFEX-I and PAFEX-II field experimental periods were simulated *post-eventum* using the meso-scale meteorological model MM5, of which the results were compared with measurements (the HOTMAC meso-scale model was also used, and for brevity only the MM5 simulations for PAFEX-I are presented here). In addition, a micro-meteorological urban flow (CFD) model was used to simulate the flow in downtown Phoenix area and its surroundings. The air quality in the Phoenix area was also studied using the USEPA's third-generation air quality modeling system (Models-3). The dispersion of motor vehicle pollutants were also studied using an upgraded version of CALINE (California Line Source Dispersion) model, CAL3HQC.

Three nested grids, using horizontal grid resolutions of 16 km, 4 km, and 1 km, were used for the MM5 simulation. The outer-most domain included the entire State of Arizona and Domain 2 covered the greater Phoenix valley, including surrounding mountains. Domain 3, the inner-most domain of the MM5, spanned only the Phoenix valley. Domain 4, where the CFD model was used, encompassed the downtown area of the City of Phoenix with a horizontal grid resolution of 50 m. Figure 20 shows the domains and the array of buildings used to mimic topography in the downtown area. For preliminary simulations discussed herein, an arbitrary array of buildings was used.

The output of the NCEP (National Center for Environmental Prediction) Eta model was used as initial and boundary values of the outer domain. The number of vertical layers of all three MM5 domains was 28, and enhanced vertical resolution near the ground was adapted to resolve the detailed structure of the boundary

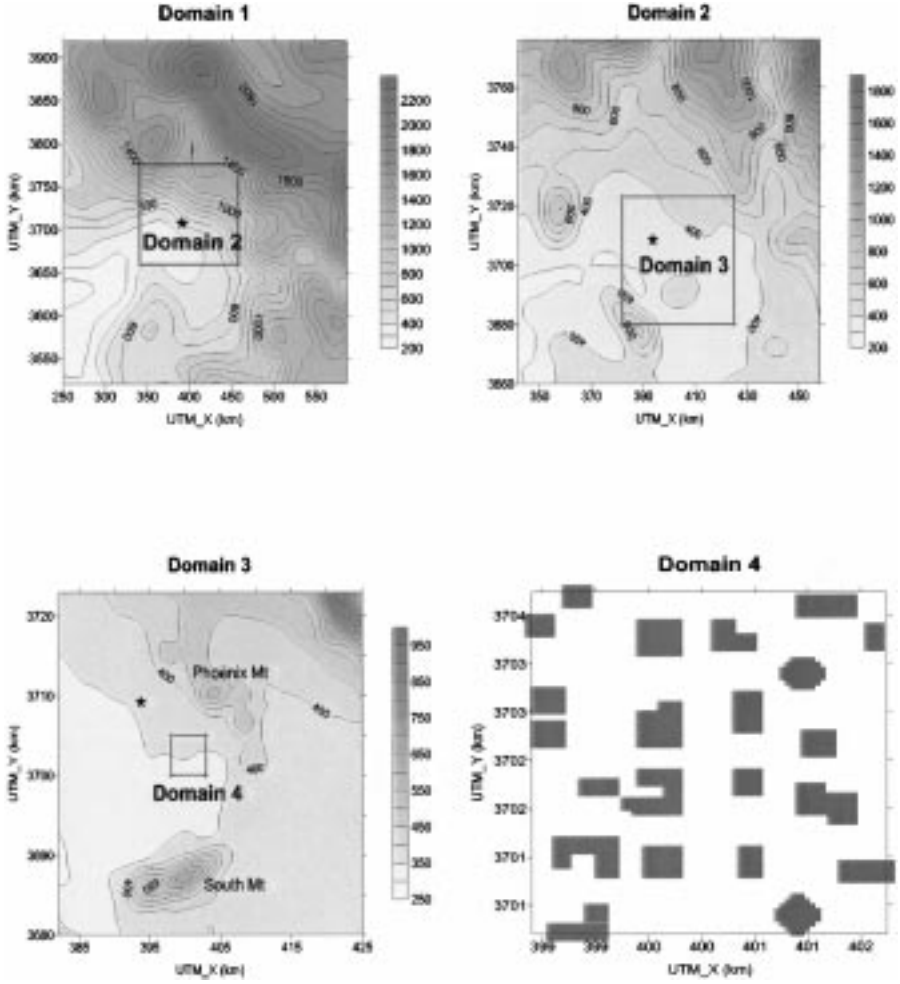

Figure 20. Computational grids used for MM5 and CFD calculations. The topography and arbitrary building geometry are represented by contours/shading. The location marked by ★ represents the PAFEX-I site where sonic anemometer measurements were made.

layer. The simulation in point was begun at 00:00 UTC January 30 (17:00 LST, January 29), 1998 and ended at 00:00 UTC February 2 (17:00 LST February 1), 1998. The horizontal distribution of simulated wind fields at approximately 10m above the ground level is shown in Figures 21(a–c) and 22(a–c), corresponding to the down slope/valley and up slope/valley wind cases, respectively. Every mountain and valley in domains 1 and 2 was well resolved and contributed to the local thermal circulation. The influence of smaller mountains, such as the Phoenix Mountains located in Domain 3, was also well resolved. Easterly flow modified by the slope/valley flow was dominant in all MM5 domains due to the fact that an anticyclonic disturbance was developing near the surface of the Northwest corner of

the outer domain although the prevailing overall synoptic wind was northwesterly. The northerly synoptic wind was too weak to affect the near-surface thermal circulation, which is typical of Phoenix climatology; consequently, valley winds are well evident in the MM5 modeling system. In Figure 23, the simulation results are compared with the wind and temperature measurements of a sonic anemometer that was located at the PAFEX-I site marked in Figure 20. The simulated near-surface temperatures of domains 1, 2, and 3 show a good agreement with the measurements. The model output also shows a reasonable agreement with the measured wind vector components, though MM5 failed to predict the detailed (minute-scale) fluctuations of real winds. The predictions based on Domain 3 showed a better agreement with the measurements toward the end of the simulation.

The CFD model used to simulate the detailed micro-meteorological fields in the urban down-town area was an incompressible, 3-dimensional anelastic equation model, originally developed by Lee and Park (1994) and modified by Baik and Kim (1999) to include a $k - \varepsilon$ turbulence closure scheme. It includes a description on thermal effects of building walls (Kim and Baik, 1999). This model was implemented with MM5 output as initial and boundary values. The number of horizontal grids in both east-west and south-north directions was 80, with a 50 m grid spacing, and the number of vertical layers was 50 with a grid spacing of 10 m (the sensitivity of results to the grid resolution remains to be investigated in future studies). A Cressman-type weighting function was used to interpolate the MM5 output of Domain 3 to the gridding of the micro-meteorological model. The forcing meteorological fields were assumed to be stationary during the 1-hour period of urban simulation. Figures 21(d) and 22(d) represent the output of this urban flow model during nocturnal and daytime periods, the mean fields of which were well simulated by MM5. (The term ‘mean field’ refers to the meteorological field computed by the larger scale model MM5). As evident from Figures 21(d) and 22(d), the model predicts complex wind patterns around the irregularly arranged group of buildings. While Figure 21(d) shows a very complicated flow pattern through the building cluster, such as flow deflection, channeling, vortex wake zones, accelerations and decelerations, such phenomena are less obvious in Figure 22(d) in view of weak mean winds present. Vortex wakes, however, are developed around some larger buildings.

5.2. AIR QUALITY MODELING IN URBAN AREAS

Owing to rapid population growth and burgeoning industrial activity, the air quality of many cities has deteriorated in recent years. It has, therefore, become necessary to use predictive tools in urban planning to ascertain the air-quality impact of land use changes (e.g., construction of freeways or recreation lakes), siting of industries and development of planned communities. Of particular interest is the increase in the number of passenger-miles and vehicle-miles traveled by urban dwellers (Bureau of Transportation Statistics, 1999), given that motor vehicular exhaust is a

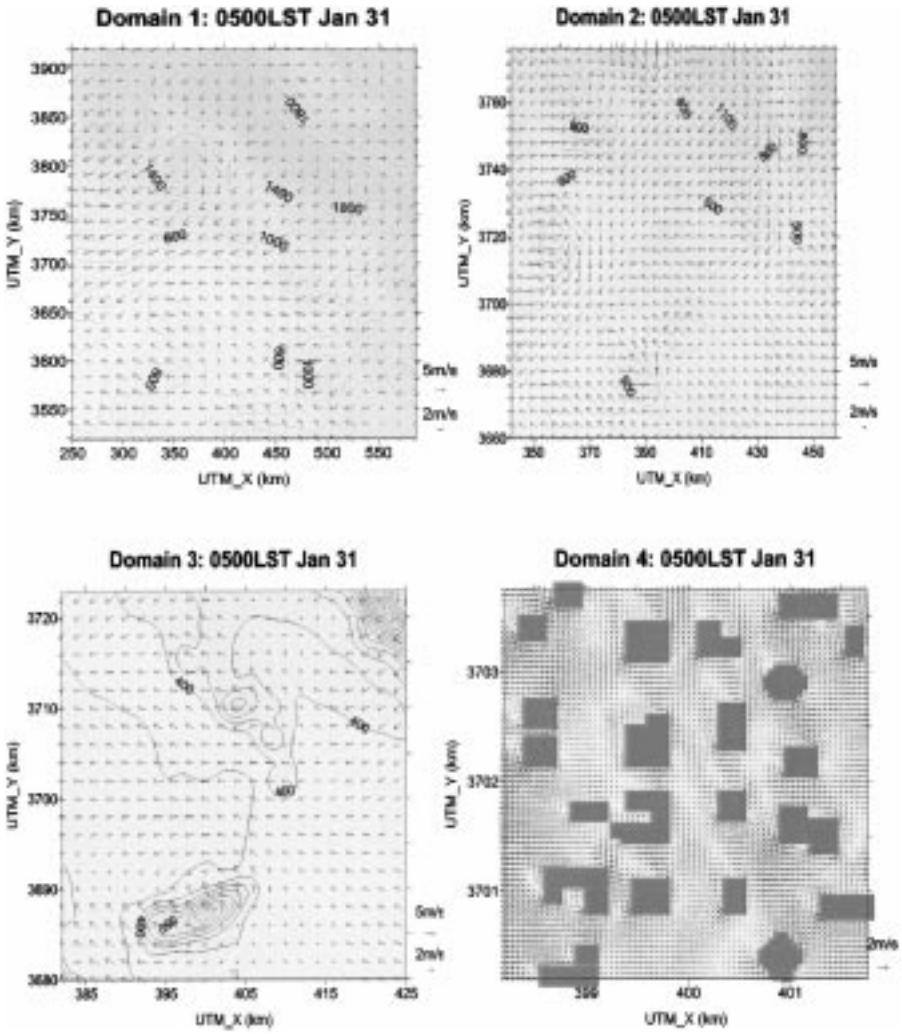

Figure 21. The distribution of horizontal wind at approximately 10m above ground level, at 05:00 LST January 31, 1998 during PAFEX-I. Results for (a) Domain 1, (b) Domain 2, (c) Domain 3, and (d) Domain 4 are shown. The shaded area represents topographical height (cf. Figure 19) and an arbitrary building array of downtown Phoenix.

major source of pollution in cities. Planners must determine whether the addition of a freeway will result in new pollution 'hot spots' due to collusion of emissions from highly congested freeways or surface street intersections and meteorological conditions.

Advanced multi-scale pollution models are being used to address air pollution issues of urban areas. The Environmental Decision Support System (EDSS) provides scientists, planners and policy makers with tools for modeling and analysis. EDSS uses several modules, including the USEPA's recently released Models-

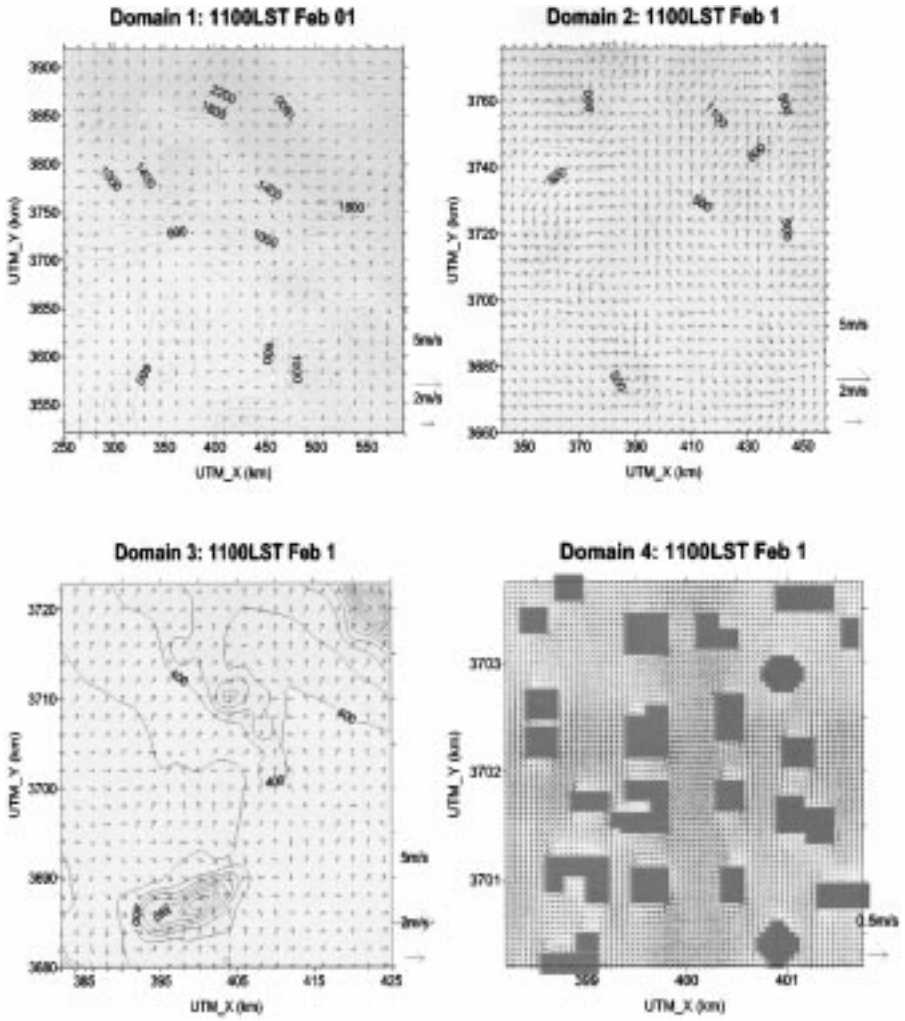

Figure 22. Same as in Figure 21, but at 11:00 LST on February 01, 1998.

3/CMAQ (Community Multiscale Air Quality Model) to provide information for making decisions on the urban to regional scale. Models-3/CMAQ is a comprehensive multiple-pollutant modeling system that encapsulates the state-of-the-science approaches to assess and predict air quality, in particular the levels of criteria pollutants. It is based on the 'one-atmosphere' modeling perspective; that is, the governing equations and computational algorithms of the air quality model are consistent and compatible with the meteorological and emission-processing models. To realize this concept, Models-3/CMAQ uses a set of comprehensive governing equations written in generalized curvilinear coordinates (Byun and Ching 1999). The aerosol module of Models-3/CMAQ considers atmospheric aerosols in three modes: coagulation, growth of particles by the addition of new mass and particle

formation. While Model-3/CMAQ can handle, interactively and simultaneously, all three phases (gas, liquid and particle) of air pollutants, the other existing air quality models only consider the dynamics and chemistry of either one or two phases. For example, the well-known antecedent of Models-3, the Urban Airshed Model (UAM; Morris and Meyers 1990), principally considers the gas phase pollutants, although some simple particle chemistry is included in it. Similarly, the Regional Acid Deposition Model (RADM; Chang *et al.*, 1987, 1990) includes the simulation of gas and liquid phase pollutants. Models-3/CMAQ has the advantages of modular structure and multiple user options, providing greater flexibility for research and regulatory applications.

Models-3 can typically resolve dispersion down to 1 km, but not to individual roads. The Transportation Analysis and SIMulation System (TRANSIMS; Nagel *et al.*, 1996) project at the Los Alamos National Laboratory attempts to simulate an entire city's individual transportation components down to individual vehicles on roads on a minute-by-minute time scale. The model first generates traffic demands based on synthesized traveler populations and consequent trip planning decisions. From this information, the congestion estimates, travel time, air quality and other dynamical system properties can be calculated. As one might expect, TRANSIMS requires immense computational resources.

For quite some time, simpler models have been used for highway dispersion at the urban scale. These models do not require the extensive databases that a code such as TRANSIMS requires, and the simpler models can be set up and run to produce quick forecasts. An example of such a working model is the CALINE, which utilizes traffic databases that includes the physical locations of roads, vehicle miles traveled, and vehicle emissions. CALINE uses a finite-line source gaussian plume model that includes atmospheric stability effects to calculate the dispersion of pollution from roads over a one-hour averaging period (for details see Benson, 1989). Predictions are made for carbon monoxide, nitrous oxide, and suspended particulate concentration. Dispersion coefficients are modified depending on stability, surface roughness, road elevation (sunken or raised highways), and thermal effects of vehicular motion. Two disadvantages of CALINE are its inability to handle complex terrain and its assumption that all pollutants are well mixed over the roadway (which may not be valid under very stable atmospheric conditions). In many of the cities of the U.S. southwest with pollution problems these assumptions are not valid.

Below, we describe the application of Models-3/CMAQ and an upgraded version of CALINE, CAL3QHZ, for the calculation of pollution concentrations in the Phoenix area. CAL3QHZ has advantages over CALINE in that it incorporates queue lengths and emission from idling vehicles. It was used to analyze localized freeway dispersion and the effect of new freeway construction in Phoenix and in particular, to estimate the effects of two new freeway segments located near previous hot spots.

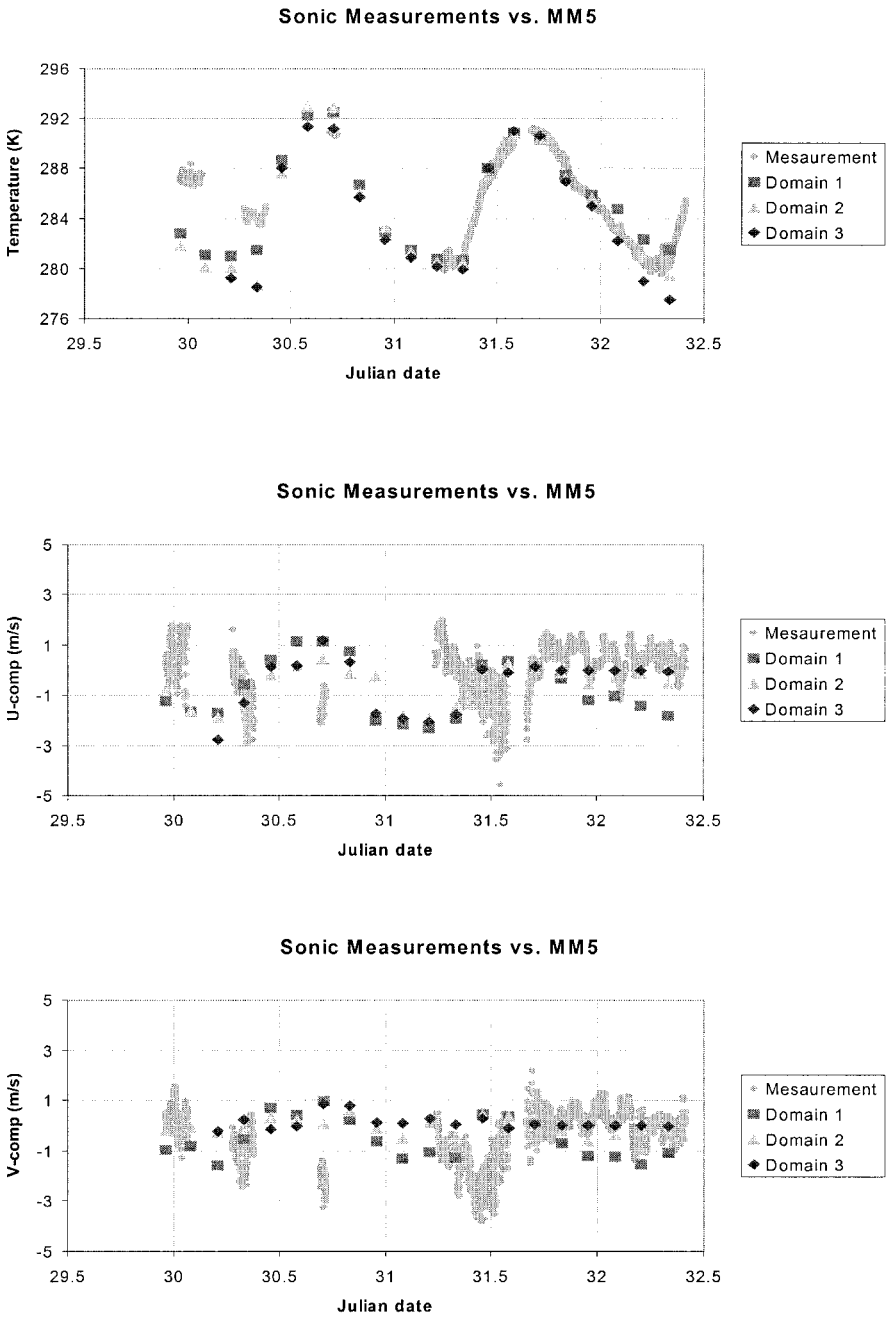

Figure 23. A comparison between time series measurements of temperature and U, V velocity measured using a sonic anemometer during PAFEX-I (shaded) with those calculated using MM5 by employing Domains 1, 2, and 3 (see symbols in the inset).

5.3. AIR QUALITY MODELING FOR PHOENIX AIRSHED

The population of the Phoenix valley has grown at the staggering pace, with a 31% increase from 1990 through 1998 (U.S. Census Bureau, 1999). Nearly 100 million vehicle miles are driven daily, requiring the planning of a large network of freeways to deal with congestion. Considering the poor air quality at present, further addition of pollution sources needs to be done with great caution and meticulous planning. For better understanding of air quality problems arising from motor vehicles and other major sources, Models-3/CMAQ modeling was carried out to simulate the air quality in the Phoenix airshed, which was extended to include existing and proposed additions to the freeway system. Emission inventory for Models-3 was developed in collaboration with the Arizona Department of Environmental Quality. For modeling the dispersion of inert pollutants from highways, emission factors were estimated using the pollution inventory MOBIL5 (Users Guide, CAL3QHC, 1994), which takes into account a variety of factors including ambient temperature, fuel properties and vehicle fleet information. The results of these simulations are summarized below.

The period July 22–23, 1996, was selected as the 'design days' of Models-3/CMAQ simulations, considering that it was a period with a high ozone episode that violated NAAQS. The computational domain spanned 120 km in east-west direction and 80 km in south-north direction, and included central Phoenix, neighboring cities and surrounding mountains. The meteorological input for Models-3/CMAQ was generated using nested MM5 simulations, with the resolution of three domains being 16 km, 4 km, and 2 km. The Models-3/CMAQ simulations were carried out with a horizontal resolution of 2 km and 28 vertical layers, as in MM5 simulations. The calculations began at 04:00 LST July 22 and ended at 00:00 LST on July 24.

Figure 24 shows the horizontal distribution of the simulated ozone concentration. Due to horizontal advection by the dominant westerly surface wind, the ozone plume is transported to the east, with the maximum concentration occurring at high elevations of the eastern Phoenix valley (cf, Section 4). Interesting enough, the NO_xconcentration in central Phoenix causes its O_3 concentration to be lower than in surrounding areas, though the traffic-induced contaminants in the proximity of central Phoenix appears to be the root cause of ozone problems in surrounding areas. As evident from Figure 25, the simulated and measured ozone concentrations show a reasonable agreement, at least qualitatively. One of the main reasons for the difference between the predicted and observed peak concentration in the afternoon of the second day is the stronger near surface winds predicted by MM5 than actually observed. The implementation of surface wind nudging in MM5 may improve the prediction of ozone concentration.

Figure 26 shows the calculated CO concentration distribution using CAL3QHZ for a typical morning rush hour based on existing major freeways (I10, I17 and state routes 60, 51 and 202) and street arterials. The meteorological conditions were

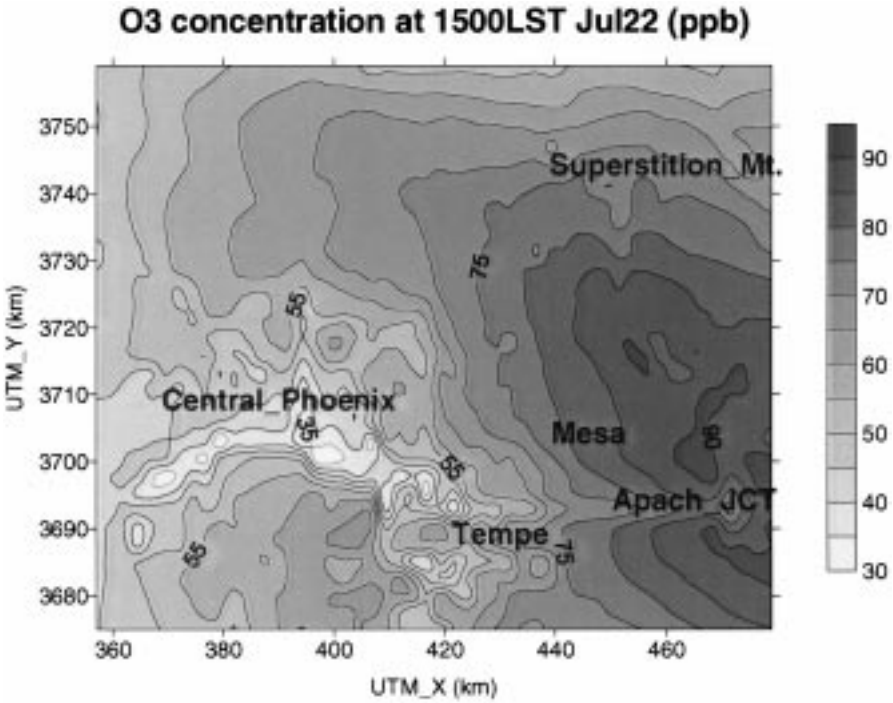

Figure 24. The horizontal distribution of simulated (using MODELS3/CMAQ system) ozone concentration in the Phoenix valley at 15:00 LST on July 22, 1996.

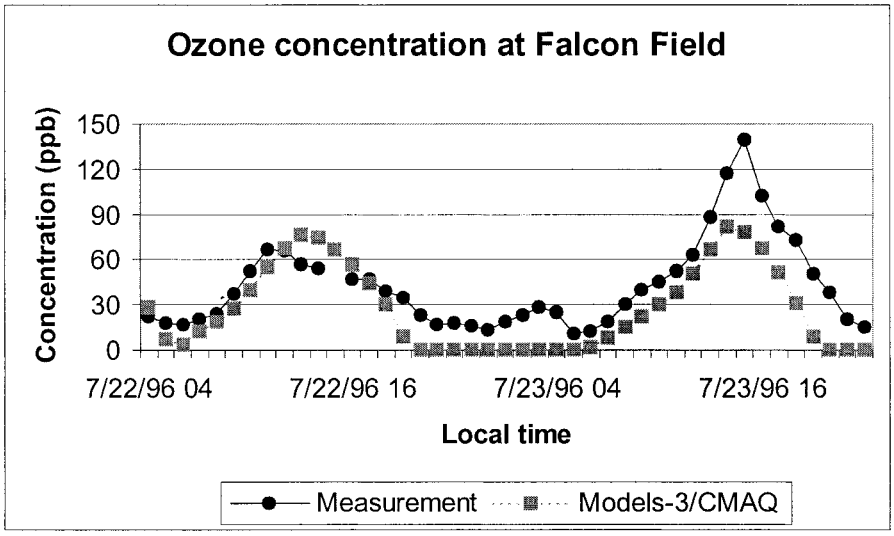

Figure 25. A comparison of simulated (Models-3/CMAQ) and measured (at the Falcon Field Airport by the Arizona Department of Environmental Quality) surface-level ozone concentration for several days in 1996.

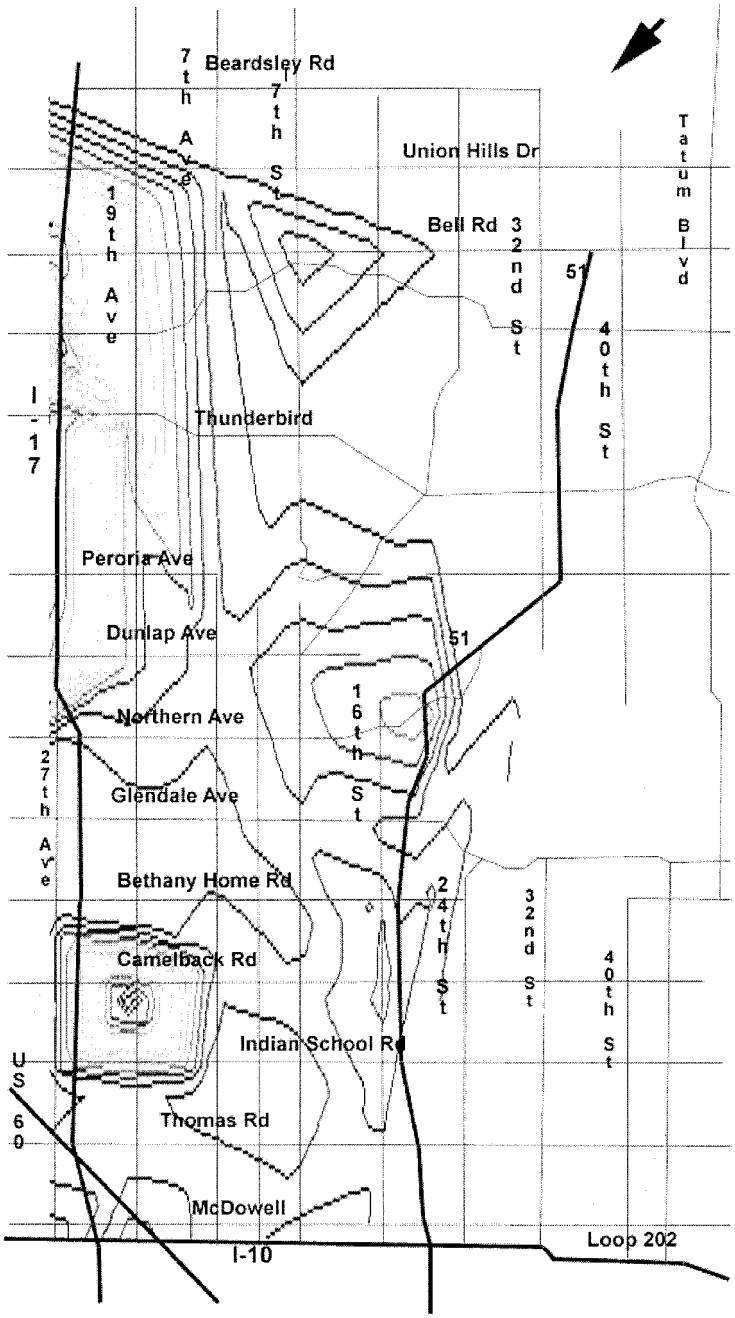

Figure 26. The calculated (using CAL3QHZ) CO concentration (indicated by contours of which the color intensity increases with the CO concentration) in the Phoenix area during the morning rush hour on January 29, 1998, using the freeway sections shown.

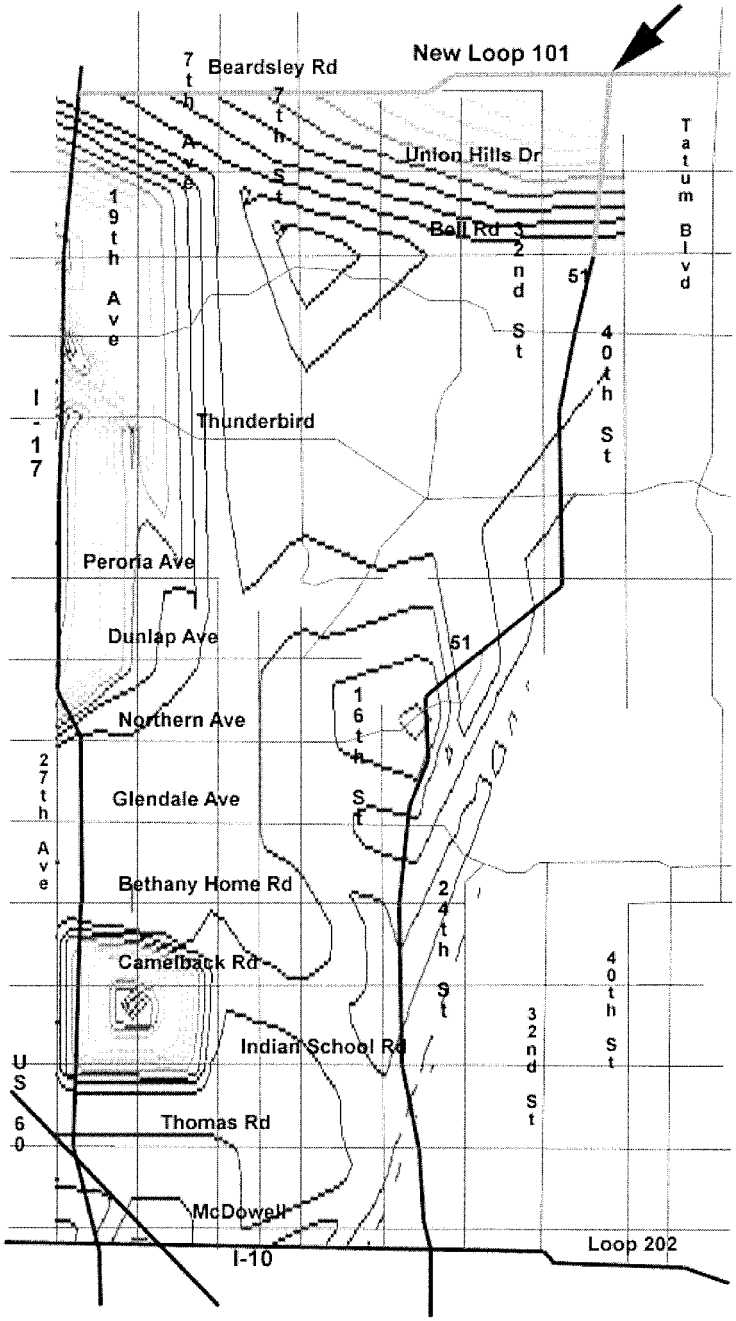

Figure 27. Same as Figure 26, but with completion of the proposed freeway AZ-101 and freeway AZ-51.

obtained from PAFEX-I on January 29, 1998 (Section 4; also see Grachev *et al.*, 1999). For this morning rush hour case, the wind was southeasterly at 2 m/s and the stability class D (slightly stable) was used. Figure 27 is a similar calculation except with the proposed addition of freeway AZ-101 (running east-west at the northern-most part of the domain) and the northern portion of AZ-51 (running north-south on the eastern-most part of the domain). In both cases, a CO hot spot due to traffic pollution was identified in the southwest portion of the domain near 19th Avenue and Camelback Road. Based on past studies (MAG, 1980), this area has been well known for its high CO pollution. Apparently the freeway addition will lead to a new hot spot at the intersection of the two freeways (see the arrow)! Kindred calculations can help planners in making decisions with regard to freeway extensions, which in this case is expected to elevate levels of CO.

6. Epitome

At the dawn of civilization, tribal communities arose to help their members face existential challenges such as the supply of food, shelter and security. With time, these communities began to focus on other aspects of life, such as culture (music, art, trading, evidence for which dates back to 10 000–30 000 years) and religion. All these attributes led to the emergence of cities (approximately 10 000 years ago), the functionality of which hinge on the simultaneous operation of a multitude of 'urban systems' such as buildings and shelter, water resources, air quality, food, security, recreation, transportation, religion and culture. In the latter part of the 20th century, a tendency to pool in larger and more sophisticated cities has evolved (e.g., mega-cities with typical populations >10 million). In 1975, 5% of the world's cities were of this type, and is expected to rise to 16% in the year 2015 (Bugliarello, 2000). Design of urban systems to cater to such mega communities will be a major challenge to humans of the 21st century, and it behooves us to develop advanced tools to design, analyze, sense, assess and secure such systems. Effective utilization of science and technology for the development of public policy governing such cities is also a necessity.

Urban Fluid Mechanics is intended to deal with urban fluid systems – air and water – which are essential components of urban infrastructure. In foregoing sections some issues related to urban air movement and their implications in microclimate, contaminant dispersion and health effects were discussed, and their study cuts across many traditional disciplines. It is hoped that this paper acts as a precursor to many future investigations on urban fluid systems, which are replete with important dynamical processes that are yet to be understood and quantified using the principals of fluid mechanics. This will undoubtedly involve advancing into new frontiers dealing with the interaction of fluid flow with biological and chemical systems of natural environments, an aspect that has received only little attention in the past. To this end, the role of multidisciplinary research cannot be overemphasized, and the current thinking focused on disciplinary research can have

only a limited impact on the rapid advancement of understanding, modeling and mitigation of urban-scale fluid flow problems.

Acknowledgements

The urban fluid mechanics research at Arizona State University (ASU) was launched in response to a University Initiative on Urban Environments, conceived and munificently supported by the Office of the Vice Provost for Research (VPR). We wish to thank VPR Jonathan Fink, Provost Milton Glick, Vice Provost Kathleen Church and Dean Peter Crouch for their encouragement and support, without which the work reported herein could not have been realized. Professors Don Boyer, Gregory Raupp and Neil Berman were instrumental in setting up the infrastructure for multidisciplinary work and numerous colleagues at ASU and visiting scientists (the list of names is too long to mention, for which we wish to apologize) are helping with our on-going work. The US National Science Foundation (NSF) has established one of its two urban Long-Term Ecological Research (LTER) sites at Arizona State University under the auspices of the Center for Environmental Studies, which acts as a valuable information resource for urban environmental studies. Since 1998, urban fluid mechanics research at ASU has been funded by the Environmental Geochemistry and Biogeochemistry (EGB) Initiative, Urban Initiative and the unsolicited grant programs of the NSF, the Arizona Department of Environmental Quality (ADEQ), Arizona Department of Transportation (ADOT), the Army Research Office (Geosciences), the Department of Energy (Environmental Meteorology) and the USEPA *via* the Southwest Center for Environmental Research and Policy (SCERP). Peter Hyde of ADEQ spent endless hours in providing technical support for air quality modeling, Estomih Kombe of ADOT provided useful technical information on Arizona highways, and Bruce Kimball of the U.S. Water Conservatory Laboratory provided Figure 4 of the paper. Professor Jong-Jin Baik kindly provided the CFD code. Invaluable help received from our ASU colleagues, Jennifer McCulley, Gabrielle Stidham, Dana Perry, Frank Yu and Destry Lucas during the preparation of this manuscript and data analysis is greatly appreciated. Editor of the Journal of Environmental Fluid Mechanics, Professor Benoit Cushman-Roisin, provided valuable guidance and comments on this paper that lead considerable improvement of its presentation.

References

B. Ackerman, The airflow program in METROMEX. In: F.A. Huff (ed.), *Summary Report*, No. 74, Ill. State Water Survey (1973) pp. 113–124.

F.A. Albini, A phenomenological model for wind speed and shear stress profiles in vegetation cover layers, *J. Appl. Meteorol.* **20** (1981) 1325–1335.

K.J. Allwine, Atmospheric dispersion in mountain valleys and basins, PNL-7922, Pacific Northwest Laboratory Report 199 (1992).

J.S. Amthor, Scaling CO_2-photosynthesis relationships from the leaf to the canopy, *Photosynthesis Res.* **39** (1994) 321–350.

J.S. Amthor, M.L. Goulden, J.W. Munger and S.C. Wofsy, Testing a mechanistic model of forest-canopy mass and energy exchange using eddy-correlation: carbon dioxide and ozone uptake by a mixed oak-maple stand, *Aust. J. Plant Physiol.* **21** (1994) 623–651.

J.R. Anderson, P.R. Buseck, T.L. Patterson and R. Arimoto, Characterization of the Bermuda tropospheric aerosol by combined individual-particle and bulk-aerosol analysis, *Atmospheric. Environ.* **30** (1996) 319–338.

J.K. Angell, W.H. Hoecker, C.R. Dickson and D.H. Pack, Urban influence on a strong daytime air flow as determined from tetroon flights, *J. Appl. Meteorol.* **12** (1973) 924–936.

S.P. Arya, *Air Pollution Meteorology and Dispersion*. Oxford University Press, Oxford (1999) 310 pp.

R. Avissar and M.M. Verstraete, The representation of continental surface processes in atmospheric models, *Rev. Geophys.* **28** (1990) 35–52.

J.J. Baik and H.Y. Chun, A dynamical model for urban heat island., *Bound. Layer Meteorol.* **83** (1997) 463–477.

J.J. Baik and J.J. Kim, A numerical study of flow and pollutant dispersion characteristics in urban street canyons, *J. Appl. Meteorol.* **38** (1999) 1576–1589.

J.J. Baik, R.S. Park, H.Y. Chun and J.J. Kim, A Laboratory model of urban street canyon flows, *J. Appl. Meteorol.* **39** (2000) 1592–1600.

S.E. Bauman, E.T. Williams, H.L. Finston, E.F. Ferrand and J. Sontowski, Street level versus rooftop sampling: carbon monoxide and aerosol in New York City, *Atmospheric. Environ.* **16** (1982) 2489–2496.

P.E. Benson, *CALINE4 – A Dispersion Model for Predicting Air Pollutant Concentrations Near Roadways*, FHWA/CA/TL-84/15 (1989).

S.E. Belcher and J.C.R. Hunt, Turbulent flow over hills and waves, *Ann. Rev. Fluid Mech.* **30** (1998) 507–538.

S.E. Belcher, D.P. Xu and J.C.R. Hunt, The response of a turbulent boundary layer to arbitrary distributed two-dimensional roughness changes, *Q. J. Roy. Meteorol. Soc.* **116** (1990) 611–635.

W.J. Beranek, General rules for the determination of wind environment. In: J.R. Pfafflin and E.N. Ziegler (eds.), *Proc. Fifth Intern. Conv. on Wind Eng.*, July, Fort Collins, CO, Vol. 2, (.), Gordon and Breach Science Publishers, New York, NY (1979).

N.S. Berman, D.L. Boyer, A.J. Brazel, S.W. Brazel, R.A. Celada, R-R. Chen, H.J.S. Fernando, M.J. Fitch and H-W Wang, Synoptic Classification and the Design of Physical Model Experiments for Complex Terrain, *J. Appl. Meteorol.* **34** (1995) 719–730.

R. Bornstein, Mean diurnal circulation and thermodynamic evolution of urban boundary layer. In: *Modeling the Urban Boundary Layer*, Am. Meteorol. Soc. (1987) pp. 53–93.

R.D. Bornstein, Observations of the urban heat island effect in New York City, *J. Appl. Meteorol.* **7** (1968) 575–582.

R.D. Bornstein and D.S. Johnson, Urban-rural wind velocity differences, *Atmospheric. Environ.* **11** (1977) 597–604.

R.D. Bornstein and T.R. Oke, Influence of pollution on urban climatology, *Adv. Environ. Sci. Engrg.* **2** (1981) 171–202.

R.D. Bornstein, P. Thunis, P. Opossi and G. Schayes, Topographic, vorticity – mode, mesoscale b (TVM) model Part II: Evaluation, *J. Appl. Meteorol.* **35** (1996) 1824–1834.

E.F. Bradley, An experimental study of the profiles of wind speed, shearing stress and turbulence at crest of a large hill, *Quart. J. Roy. Meteorol. Soc.* **106** (1980) 101–123.

W.F. Bradley, A micrometeorological study of velocity profile and surface drag in the region modified by a change in surface roughness, *Q. J. Roy. Meteorol. Soc.* **94** (1968) 361–329.

J. Brechling and H. Ihlenfeld, The modeling of the atmospheric boundary layer in a wind tunnel with an open test section and its application for investigations of the flow around buildings. In: R.J.

Perkins and S.E. Belcher (eds.) *Flow and Dispersion Through Groups of Obstacles*. Claredon Press, New York (1997) pp. 71–88.

G.A. Briggs, Diffusion modeling with convective scaling and effects of surface inhomogeneities. In: *Modeling the Urban Boundary Layer*, Am. Meteorol. Soc. (1987) pp. 297–333.

G.A. Briggs, R.S. Thompson and W.H. Snyder, Dense gas removal from a valley by cross winds, *J. Haz. Mat.* **24** (1990) 1–38.

P.W.M. Brighton, Strongly stratified flow past three-dimensional obstacles, *Q. Jour. Roy. Meteorol. Soc.* **104** (1978) 289–307.

R.E. Britter and J.C.R. Hunt, Velocity measurements and order of magnitude estimates of the flow between two buildings in a simulated atmospheric boundary layer, *J. Indust. Aerodynamics* **4** (1979) 165–182.

M. Brown, M. Leach, J. Reisner, D. Stevens, S. Smith, S. Chin, S. Chan and B. Lee, Numerical modeling from mesoscale to urban scale to building scale, *Proc. 3rd Symposium on the Urban Environment*, 14–18 August, Davis, CA. (2000) pp. 64–65.

W. Brutsaert, Heat and mass transfer to and from surfaces with dense vegetation or similar permeable roughness, *Boundary Layer Meteorol.* **16** (1979) 365–388.

G. Bugliarello, Rethinking Today's Cities – Designing Tomorrows Urban Centers, Paper presented at the Technical Symposium on Earth Systems Engineering, National Academy of Engineering, Washington DC, October 24 (2000).

Bureau of Statistics, U.S. Department of Transportation, The National Transportation Statistics (1999).

D.W. Byun and J.K.S. Ching, *Science algorithms of the EPA models-3 Community Multiscale Air Quality (CMAQ) modeling system*, EPA/600/R-99/030, U.S. EPA (1999).

R.E. Carbone, Atmospheric observations in weather prediction. In: R.E. Pielke and Sr. R.E. Pielke *Storms*, Vol 1, Routledge Press, London (2000).

I.P. Castro, A. Kumar, W.H. Snyder and S.P.S. Arya, Removal of slightly heavy gases from a valley by crosswinds, *J. Haz. Mat.* **34** (1993) 271–293.

S.J. Caughey, J.C. Wyngaard and J.C. Kaimal, Turbulence in the evolving stable boundary layer, *J. Atmospheric. Sci.* 36 (1979) 1041–1052.

J.E. Cermak, D.J. Lombardi and R.S. Thompson, Applications of physical modeling to the investigation of air pollution problems in urban areas, presented at *67th Annual Meeting of Air Poll. Control Assoc.*, June 9–13, Denver, CO. APCA paper # 74–160 (1974).

S.T. Chan, D.E. Stevens and R.L. Lee, A model for flow and dispersion around buildings and its validation using laboratory measurements, *Proc. 3rd Symposium on the Urban Environment, 14–18 August*, Davis, CA. (2000) pp. 56–57.

J.S. Chang, R.A. Brost, I.S.A. Isaksen, S. Madronich, P. Middleton, W.R. Stockwell and C.J. Walcek, A three-dimensional Eulerian acid deposition model: Physical concepts and formulation, *J. Geophy. Res.* **92** (1987) 14681–14700.

J.S. Chang, P.B. Middleton, W.R. Stockwell, C.J. Walcek, J.E. Pleim, H.H. Landsford, S. Madronich, F.S. Binkowski, N.L. Seaman and D.R. Stauffer, The Regional acid deposition model and engineering model, NAPAP SOS/T Report 4, in National Acid Precipitation Assessment Program: State of Science and Technology, Volume 1, National Acid Precipitation Program, 722 Jackson Place, N. W., Washington, D.C. September (1990).

S.A. Cheatham, B.Z. Cybyk and J.P. Boris, Simulation of fluid dynamics around a cubical building, *Proc. 3 Symposium on the Urban Environment*, 14–18 August, Davis, CA. (2000) pp. 46–47.

J.K.S. Ching, J.M. Godowitch and J.F. Clarke, Urban scale variations of turbulent energy fluxes, Presented *at AMS Specialty Conf. on Air Quality Modeling of the Nonhomogeneous, Nonstationary Urban Boundary Layer*, Oct. 31–Nov. 4, Baltimore, MD (1983).

R.M. Cionco, A mathematical model for air flow in a vegetative canopy, *J. Appl. Meteorol.* **4** (1995) 517.

R.M. Cionco, Design and execution of Project WIND. In: *Proc 19th Conference of Agricultural and Forest Meteorology (Charleston)*, American Meteorology Society, Boston, MA (1989).

R.N. Cionco and others, An overview of MADONA: a multinational field study of high resolution meteorology and diffusion over complex terrain, *Bull. Am. Met. Soc.* **80** (1999) 5–19.

J.S. Cole and H.J.S. Fernando, Some aspects of the decay of convective turbulence, *Fluid Dyn. Res.* **23** (1998) 167–176

J.P. Collins, A. Kinzig, N.B. Grimm, W.F. Fagan, D. Hope, J. Wu and E.T. Borer, A new urban ecology. *Am. Sci.* **88** (2000) 416–425.

R.L. Coulter, A case study of turbulence in the stable Nocturnal Boundary Layer, *Boundary-Layer Meteorol.*, **52** (1990) 75–92.

C.F. Cox, B.Z. Cybyk, J.P. Boris, Y.T. Fung and S.W. Chang, Coupled microscale-mesoscale modeling of contaminant transport in urban environments, *Proc. 3rd Symposium on the Urban Environment*, 14–18 August, Davis, CA. (2000) pp. 66–67.

W.F. Dabberdt, F.L. Ludwig and W.B. Jr. Johnson, Validation and applications of an urban diffusion model for vehicular pollutants, *Atmospheric. Environ.* **7** (1973) 603–618.

W.F. Dabberdt, J. Hales, S. Zubrick, A. Cook, W. Krajewski, J.C. Doran, C. Mueller, C. King, R.N. Keener, R. Bornstein, D. Rodenhuis, P. Kocin, M.A. Rossetti, F. Sharrocks, E.M., Sr., Stanley, Forcast Issues in the Urban Zone: Report of the 10th prospectus Development Team of the U.S. Weather Research Program, *Bull. Amer. Meteorol. Soc.* **81** (2000) 2047–2064.

B. Davidson and P.K. Rao, Experimental studies of the valley-plainwind, *Int. J. Air Water Pollu.* **7** (1963) 907–923.

I.P.D. De Silva, A. Brandt, L.J. Montenegro and H.J.S. Fernando, Gradient Richardson number measurements in a stratified shear layer, *Dyn. Atmospheric. Oceans.* **30** (1979) 47–63.

D.G.G. De Pury and G.D. Farquhar, Simple scaling of photosynthesis from leaves to canopies without the errors of big-leaf models, *Plant, Cell and Environ.* **20** (1997) 537–557.

J.W. Deardorff, Convective velocity and temperature scales for the unstable planetary boundary layer and for Rayleigh convection, *J. Atmospheric. Sci.* **27** (1970) 1211–1213.

J.W. Deardorff, Mixed-layer entrainment: A review. In: J.C. Weil (ed.) *7th Symposium on Turbulence and Diffusion.*, Am. Meteorol. Soc. (1985) pp. 39–42.

J.W. Deardorff, G.E. Willis and D.K. Lilly, Laboratory investigation of non-steady penetrative convection, *J. Fluid Mech.* **35** (1969) 7–31.

J.W. Deardoff, G.E. Willis and B.H. Stockton, Laboratory studies of the entrainment zoone of a convectively mixed layer, *J. Fluid Mech.* **100** (1980) 41–64.

W. Debler and S.W. Armfield, The purging of saline water from rectangular and trapezoidal cavities by an overflow of turbulent sweet water, *J. Hydr. Res.* **35** (1997) 43–62.

H. Derbyshire, Stable boundary layers: observations, models and variability, Part I: Modeling and measurements, *Boundary-Layer Meteorol.* **74** (1995a) 19–54.

H. Derbyshire, Stable boundary layers: observations, models and variability Part II: Data analysis and averaging effects, *Boundary-Layer Meteorol.* **75** (1995b) 1–24.

S.H. Derbyshire, Nieuwstadt's stable boundary layer revisited, *Q. J. Roy. Meteorol. Soc.* **116** (1990) 127–158.

M.H. Dickerson, Mascon – A mass consistent atmospheric flux model for regions with complex terrain, *J. Appl. Meteorol.* **17** (1978) 241–253.

M.H. Dickerson and P.H. Gudiksen, Atmospheric studies in complex Terrain, Tech Progress Report FY-1979 through FY-1983, ASCOT 84–1/UCID-19851, U. S. Dept. of Energy, *Lawrence Livermore Natl. Lab.*, Livermore, CA (1984).

R.E. Dickinson, A.N. Hahmann and Q. Shao, Commentary on Mecca sensitivity studies. In: Howe W and Henderson-Sellers A (Eds.) *Assessing Climate Change.* Sidney: Gordon and Breach Science Publishers (1997) pp. 195–206.

Doran, J.C., 1991: The effects of ambient winds on valley drainage flows, *Boundary-Layer Meteorol.*, 55, 177–189.

J.C. Doran, T.W. Horst and C.D. Whiteman, The development and structure of nocturnal slope winds in a simple valley, *Boundary-Layer Meteorol.* **52** (1990) 41–68.

J. Dudhia, D. Gill, Y-R. Guo, K. Manning, W. Wang and J. Chiszar, *PSU/NCAR Mesoscale modeling system tutorial class notes and user's guide: MM5 modeling system version 3*, NCAR (2000).

F. Ellefsen, A fine resolution urban terrain characteristics database of greater St. Louis, Missouri. STAS Report for U.S. Army Research Laboratory-BED, Contact: R.M. Cionco at USARL-BED, Adelphi, MD, USA (1993).

W.P. Elliot, The growth of the atmospheric internal boundary layer, *Trans. Am. Geophys. Union*, **39** (1958) 1048–1054.

A.W. Ellis, M.L. Hilderbrandt and H.J.S. Fernando, Evidence of lower atmospheric ozone 'sloshing' in an urban valley, *Phys. Geogr.* **20** (1999) 520–536.

A.W. Ellis, M.L. Hilderbrandt, W. Thomas and H.J.S. Fernando, A case study of the climatic mechanisms contributing to the transport of lower atmospheric ozone across metropolitan Phoenix area, *J. Climate Res.* **15** (2000) 13–31.

T.H. Ellison and J.S. Turner, Turbulent entrainment in stratified flows, *J. Fluid Mech.* **6** (1959) 423–448.

M.H. Emery, A.Y. Chtchelkanova, B.Z. Cybyk, J.P. Boris, J.H. Shinn and F.J. Bouveia, Detailed modeling of air flow around a complex building, *Proc. 3rd Symposium on the Urban Environment*, 14–18 August, Davis, CA. (2000) 48–49.

J.D. Fast, J.C. Doran, W.J. Shaw, R.L. Coulter and T.J. Martin, The evolution of the boundary layer and its effect on air chemistry in the Phoenix area. *J. Geophys. Res.* **105** (2000) 22,833–22,848.

G.D. Farquhar and S. von Caemmerer, Modelling of photosynthetic response to environmental conditions. In: Lange OL, Noble PS, Osmond, CB, Ziegler H (Eds.), *Physiological Plant Ecology II, Encycl. Plant Phys.* (1982) pp. 549–587, Berlin, Springer-Verlag.

C. Freytag, MERKUR-results: aspects of the temperature field and the energy budget in a large alpine valley during mountain and valley wind, *Contrib. Atmospheric. Phys.* **58** (1985) 458–476.

C. Freytag, Results from the MERKUR experiment: Mass budget and vertical motions in a large valley during mountain and valley wind, *Meteorol. Atmospheric. Phys.* **37** (1987) 129–140.

H.J.S. Fernando, Turbulent mixing in stratified fluids, *Ann. Rev. Fluid Mech.* **23** (1991) 455–493.

H.J.S. Fernando, Migration of density interfaces subjected to differential turbulent forcing, *Geophys. Astrophys. Fluid Dyn.* **78** (1995) 1–20.

H.J.S. Fernando and J.C.R. Hunt, Some aspects of turbulence and mixing in stably stratified fluids, *Dyn. Atmospheric. Oceans* **23** (1996) 35–62.

J.J. Finnigan and P.J. Mulhearn, Modeling waving crops in a wind tunnel, *Bound. Layer Meteorol.* **14** (1978) 253–277.

S. Galmarini, C. Beets, P.G. Duynkerke and J. Vila-Guerau De Arellano, Stable nocturnal boundary layers: A comparison of one-dimensional and large-eddy simulation models, *Boundary-Layer Meteorol.* **88** (1998) 181–210.

J. Gandemer, Inconfort du au vent aux abords des batiments: concepts aerodynamiques, cahiers du centre scientifique et technique du batiment, No. 170, Cahier 1384. C.S.T.B., Nantes, France. Also Avail. in Translation as NBS Tech. Note 710–719, March 1978 (1976) 48 pp

J.R. Garratt, Review: the atmospheric boundary layer, *Earth-Science Rev.* **37** (1994) 89–134.

S. Goldstein, Wakes. Ch. XIII. In: *Modern Developments In Fluid Dynamics*, 11, Dover Publications, New York, NY (1965) pp. 548–600.

W. Gong, P.A. Taylor and A. Dornbrack, Turbulent boundary-layer flow over fixed aerodynamically rough two-dimensional sinusoidal waves, *J. Fluid Mech.* **312** (1996) 1–37.

A.A. Grachev, H.J.S. Fernando, J.C.R. Hunt, E.P. Pardyjak, I. Oroud, N.S. Berman, F. Yu and G. Wang, The structure of the atmospheric boundary layer over the complex terrain of Phoenix valley, *Proc. of the 13th Symposium on Boundary Layers and Turbulence*, 79th AMS Meeting, Jan. 10–15, Dallas, Texas (1999) pp. 331–334.

A.L.M. Grant, An observation study of the evening transition boundary-layer, *Q. J. Roy. Meteorol. Soc.* **123** (1997) 657–677.

G.A. Grell, J. Dudhia and D.R. Stauffer, *A Description of the Fifth-Generation Penn State/NCAR Mesoscale Model (MM5)*, NCAR Technical Note, NCAR/TN-398+STR (1994) pp. 122.

S. Grossman-Clarke, B.A. Kimball, D.J. Hunsaker, S.P. Long, R.L. Garcia, T. Kartschall, G.W. Wall, P.J., Jr Pinter, F. Wechsung and R.L. LaMorte, Effects of elevated CO_2 on canopy transpiration in senescent spring wheat, *Agr. Forest Meteorol.* **93** (1999) 95–109.

H. Hanazaki, A numerical study of nonlinear waves in a transcritical flow of stratified fluid past an obstacle, *Phys. Fluidsm.* **A4** (1999) 2230–2243.

S.R. Hanna, Urban diffusion problems. Ch. 6 in *Lectures on Air Pollution and Environmental Impact Analyses*, D. A. Haugen, Coord., Amer. Meteorol. Soc., Boston, MA (1975) 209–227.

S.R. Hanna and D.G. Strimaitis, Rugged terrain effects on diffusion. In: *Atmospheric Process Over Complex Terrain, Meteorol. Monogr.*, 23, Amer. Meteorol. Soc., Boston, MA (1990) pp. 109–142.

S.R. Hanna, G.A. Briggs and R.P. Jr., Hosker, *Handbook on Atmospheric Diffusion.* U.S. Dept. of Energy Tech. Info. Center, Oak Ridge, TN, DOE/TIC-11223. Avail. NTIS, Springfield, VA, as DE82002045 (1982) 102 pp.

S.L. Heisler, P. Hyde, M. Hubble, F. Keene, G. Neuroth, M. Ringsmuth, and W.R. Oliver, *Reanalysis of the metropolitan Phoenix voluntary early ozone plan (VEOP)*. ENSR Document 0493–014–710 (1997).

B. Hennemuth, Temperature field and energy budget of a small Alpine valley, *Contrib. Atmospheric. Phys.* **58** (1985) 545–559.

B. Hennemuth, Thermal asymmetry and cross-valley circulation in a small alpine valley, *Boundary Layer Meteorol.* **36** (1986) 371–394.

B. Hennemuth and U. Kohler, Estimation of the energy balance of the Dischma Valley, *Arch. Meteorol. Geophys. Bioklimatol.* **Ser.B34** (1984) 97–119.

A.W. Hogan, and M.G. Ferrick, Observations in nonurban heat islands, *J. Appl. Meteorol.* **37** (1997) 232–236.

A.A.M. Holstag and F.T.M. Nieuwstadt, Scaling the Atmospheric Boundary Layer, *Boundary-Layer Meteorol.* **36** (1986) 201–209.

T.W. Horst, K.J. Allwine and C.D. Whiteman, A thermal energy budget for nocturnal drainage flow in a simple valley, Preprints, *Fourth Conf. on Mountain Meteorology*, Seattle, WA, American Meteorology Society (1987) pp. 15–19.

T.W. Horst, D.C. Bader and C.D. Whiteman, Comparison of observed and simulated nocturnal valley thermal energy budgets, *Proc. Int. Conf. On Mountain Meteorology and ALPEX*, Garmisch-Partenkirchen, Germany, Germ. Meteorol. Soc. (1989) pp. 127.

R.P. Jr. Hosker, Empirical estimation of wake cavity size behind block-type structures, In Preprints of *Fourth Symposium on Turb., Diff. and Air Poll.*, Jan. 15–18, Reno, NV, Am. Meteorol. Soc., Boston, MA (1979) pp. 92–107.

R.P. Jr. Hosker, Flow and dispersion near obstacles. In: D. Randerson, (Ed.), Ch. 7 of *Atmospheric Science and Power Production*, U.S. Dept. Energy, Tech. Info. Center, DOE/TIC – 2760 (DE 84005177), Oak Ridge, TN (1984).

R.P. Jr. Hosker, The effects of buildings on local dispersion. In: Modeling the Urban Boundary Layer, *Am. Meteorol. Soc.* (1987) pp. 95–159.

W.G. Hoydysh, R.A. Griffiths and Y. Ogawa, A scale model study of the dispersion of pollution in street canyons. Presented at 67th *Annual Meeting of Air Poll. Control Assoc.*, June 9–13, Denver, CO. APCA (1974).

A. Huber, M. Bolstad, M. Freeman, S. Rida, E. Bish and K. Kuehlert, Addressing human exposures to air pollutants around buildings in urban areas with computational fluid dynamics (CFD) models, 3rd *Symposium on the Urban Environment*, 14–18 August, Davis, CA. (2000) pp. 62–63.

J.C.R. Hunt, Diffusion in the stably stratified atmospheric boundary layer, *J. Clim. App. Meteorol.* **24** (1985) 1187–1195.

J.C.R. Hunt, How cities will look in the 21st century? Habitat II Conference, Publisher: United Nations Center for Regional Development, Nagoya, Japan (1996).

J.C.R. Hunt and J.E. Simpson, Atmospheric boundary layers over non-homogeneous terrain. In: E. Plate (ed.), Ch. 7 of *Engineering Meteorol.*, Elsevier (1982) pp. 269–318.

J.C.R. Hunt, J.C. Kaimal, J.E. Gaynor, Some observations of turbulence structure in stable layers, *Q. J. Roy. Meteorol. Soc.* **111** (1985) 793–815.

J.C.R. Hunt, Y. Feng, P.F. Linden, M.D. Greenslade and S.D. Mobbs, Low- Froude-number stable flows past mountains, *Il Nuovo Cimento* **20C** (1997) 261–272.

J.C.R. Hunt, H.J.S. Fernando, A.A. Grachev, E.P. Pardyjak, N.S. Berman, and F. Yu, Slope-breezes and weak air movements in a wide enclosed valley, submitted for publication (2000).

T. Hussain and B.E. Lee, A wind tunnel study of the mean pressure forces acting on large groups of low rise buildings, *J. Wind Ind. Aerodyn.* **6** (1980) 207–225.

S.B. Idso, Non-water stressed baselines: a key to measuring and interpreting plant water stress, *Agr. Forest Meteorol.* 24 (1982) 45–55.

IGPO, Land Surface Parameterizations/ Soil-Vegetation-Atmosphere-Transfer Schemes Workshop. IGPO Publication Series 31 (1997).

N. Isyumov and A.G. Davenport, The ground level wind environment in built-up areas, Proc. Fourth International Conference on Wind Effects on Buildings and Structures, September 8–12, 1977, Heathrow, Cambridge University Press, London (1975) pp. 403–422.

P.S. Jackson and J.C.R. Hunt, Turbulent wind flow over low hills, *Q. J. Roy Meteorol. Soc.* **101** (1975) 929–955.

C.M.J. Jacobs and H.A.R. De Bruin, The sensitivity of regional transpiration to land-surface characteristics: significance of feedback, *J. Climate* **5** (1992) 683–698.

P.G. Jarvis and K.G. McNaughton, Stomatal control of transpiration: scaling up from leaf to region, *Adv. Ecological Res.* **15** (1986) 1–49.

N. Jerram, S.E. Belcher and J.C.R. Hunt, Turbulent flow through a distributed force – a model for the wind within and above an urban canopy. In: R.J. Perkins and S.E. Belcher, (eds.) *Flow and Dispersion through Group of Obstacles*. Clarendon Press, London (1997) pp. 157–175.

N. Jerram, J.R. Perkins, J.C.H. Fung, M.J. Davidson, S.E. Belcher and J.C.R. Hunt, Atmospheric flow through groups of buildings and dispersion from localized sources. In: J.E. Cermak, A. D. Davenport, E.J. Plate, and D.X. Viegas (eds.), *Wind Climate In Cities*. Kluwer Academic Publishers, Dordrecht (1994) pp. 109–130.

W.B. Johnson, R.C. Sklarew and D.B. Turner, Urban air quality simulation modeling. In: A. C. Stern, (ed.), Ch. 10 of *Air Pollution*, third edition, Vol. I. Academic Press, New York, NY (1976) pp. 503–562.

W.B. Johnson, F.L. Ludwig, W.F. Dabberdt and R.J. Allen, An urban diffusion simulation model of carbon monoxide, *J. Air Pollut. Control Assoc.* **23** (1973) 490–498.

R. Joumard, Ausbreitungsmodelle Fur Verkehrs-Immissionen. In: K. Hoffman, P. Leisen, and H. Waldemeyer, (eds.) Strassenschluchten undVergleich zu franzosischen Messungen, Abgasbelastungen durch den Kraftfahrzeugverkehr, TUV Rhineland, Germany (1982) pp. 187–203.

J.C. Kaimal, Turbulence spectra, length scales and structure parameters in the stable surface layer, *Boundary-Layer Meteorol.* **4** (1972) 290–309.

J.C. Kaimal, J.C. Wyngaard, D.A. Haugen, O.R. Cote, Y. Izumi, S.J. Caughey, and C.J. Readings, Turbulence structure in the convective boundary layer, *J. Atmospheric. Sci.* **33** (1976) 2152–2169.

J.C. Kaimal and J.J. Finnigan, *Atmospheric Boundary Layer Flows*, Oxford University Press (1994).

H. Kaplan and N. Dinar, A Lagrangian dispersion model for calculating concentration distribution within a built-up domain, *Atmospheric. Environ.* **30** (1996) 4197–4207.

T. Kawatani and R.N. Meroney, Turbulence and wind speed characteristics within a model canopy flow field, *Agr. Meteorol.* 7 (1970) 143–158.

J.J. Kim and J.J. Baik, A numerical study of thermal effects on flow and pollutant dispersionin urban street canyons, *J. Appl. Meteorol.* 38 (1999) 1249–1261.

B.A. Kimball, R.L. LaMorte, P.J. Jr. Pinter, G.W. Wall, D.J. Hunsaker, F.J. Adamsen, S.W. Leavitt, T.L. Thompson, A.D. Matthias and T.J. Brooks, Free-air CO2 enrichment and soil nitrogen effects on energy balance and evapotranspiration of wheat, *Water Res. Res.* 35 (1999) 1179–1190.

J.C. Klewicki, J.F. Foss and J.M. Wallace, High Reynolds number boundary layer turbulence in the atmospheric surface layer above westerns Utah's salt flata. In: Donnelly, R.J. and Sreenivasan, K.R. (eds.) Flow in Ultra High Reynolds and Rayleigh Numbers: A Status Report., Springer Verlag (1998) pp. 450–458.

J. Kondo, T. Kuwagata and S. Haginoya, Heat budget analysis of nocturnal cooling and daytime heating in a basin, *J. Atmospheric. Sci.* **46** (1989) 2917–2933.

S. Kotaki and T. Sano, Simulation model of air pollution in complex terrains including streets and buildings, *Atmospheric. Environ.* 15 (1981) 1001–1009.

R.A. Kropfli and N.M. Kohn, Persistent horizontal rolls in the urban mixed layer as revealed by dual-Doppler radar, *J. Appl. Meteorol.* **17** (1978) 669–676.

V.P. Kukharets and L.R. Tsvang, Atmospheric turbulence characteristics over temperature-inhomogeneous land surface, Part I: Inhomogeneities of land surface temperature, *Bound. Layer Meteorol.* 86 (1998) 89–101.

T. Kuwagata and F. Kimura, F., Daytime boundary layer evolution in a deep valley, Part II: Numerical simulation of the cross-valley circulation, *J. Appl. Meteorol.* **36** (1997) 883–895.

J.P. L'homme and B. Monteny, Theoretical relationship between stomatal resistance and surface temperatures in sparse vegetation. *Agr. Forest Meteorol.* **104** (2000) 119–131.

I.Y. Lee and H.M. Park, Parameterization of the pollutant transport and dispersion in urban street canyons, *Atmospheric. Environ.* **29** (1994) 2343–2349.

R.L. Lee, R.J. Calhoun, S.T. Chan, J. Jr. Leone, J. Shinn and D.E. Stevens, Urban dispersion CFD modeling, Fact or Fiction?, *3rd Symposium on the Urban Environment*, 14–18 August, Davis, CA. (2000) pp. 54–55.

R. Leuning, F.X. Dunin and Y.P. Wang, A two-leaf model for canopy conductance, photosynthesis and partitioning of available energy. II. Comparison with measurements. *Agr. Forest Meteorol.* **91** (1998) 113–125.

R. Leuning, F.M. Kelliher, D.G.G. De Pury and E.D. Schulze, Leaf nitrogen, photosynthesis, conductance and transpiration: scaling from leaves to canopies. *Plant Cell Environ.* **18** (1995) 1183–1200.

Y-L. Lin and R.B. Smith, Transient dynamics of airflow near a local heat source, *J. Atmospheric. Sci.* **43** (1986) 40–49.

E. Jr. Logan and D.S. Barber, *I, Effect of lateral spacing on wake characteristics of buildings, NASA Contractor Report* CR-3337, Avail. NTIS, Springfield, VA (1980) 74 pp.

J. Lu, S.P. Arya, W.H. Synder and R.E. Jr. Lawson, A laboratory study of the urban heat island in a calm and stably stratified environment, Part I: Temperature field, *J. Appl. Meteorol.* **36** (1997a) 1377–1391.

J. Lu, S.P. Arya, W.H. Synder and R.E. Jr. Lawson, A laboratory study of the urban heat Island in a calm and stably stratified environment, Part II: Velocity field, *J. Appl. Meteorol.* **36** (1997b) 1392–1402.

R. Lu and R.P. Turco, Air pollution transport in a coastal environment. Part 1: Two dimensional simulations of sea breeze and mountain effects. *J. Atmospheric. Sci.* **51** (1994) 2285–2308.

F.L. Ludwig and J.H.S. Kealoha, Urban climatological studies, Final Report, Contract CODS-DAHC-20–67–C-0136, Stanford Res. Instit., CA (1968).

R.W. Macdonald, Modeling the mean velocity profile in the urban canopy layer. *Bound. Layer Meteorol.* **97** (2000) 25–45.

MAG, Maricopa Association of Governments, *Carbon Monoxide Hot Spot Analysis in the Phoenix Urban Area, Report*, # T133–80–4, Maricopa Association of Governments Transportation and Planning Office (1980).

L. Mahrt, Relation of slope winds to the ambient flow over gentle terrain, *Boundary-layer Meteorol.* **53** (1990) 93–102.

L. Mahrt, Stratified atmospheric boundary layers and breakdown of models, *Theor. Comp. Fluid Dynamics* **11** (1998) 263–279.

Y.S. Malhi, The significance of the dual solutions for heat fluxes measured by the temperature fluctuation method in stable conditions, *Boundary-Layer Meteorol.* **74** (1995) 389–396.

M. Maki, T. Harimaya and K. Kikuchi, Heat budget studies on nocturnal cooling in a basin, *J. Meteorol. Soc. Japan* **64** (1986) 727–740.

P.J. Mason and J.C. King, Measurements and predictions of flow and turbulence over an isolated hill of moderate slope, *Q. J. Roy. Meteorol. Soc.* **111** (1985) 627–640.

P.J. Mason and R.I. Sykes, Flow over an isolated hill of moderate slope, *Q. J. Roy. Meteorol. Soc.* **105** (1979) 385–395.

K. McKeen, Taming the city's man-made winds. *Discover* **5** (1984) 94–97

J.L. McNaughton and P.G. Jarvis, Predicting effects of vegetation changes on transpiration and evaporation. In: Kozlowski, T.T. (ed.) *Water Deficits and Plant Growth.*, New York Academic Press. (1983) pp. 1–47.

K.G. McNaughton and P.G. Jarvis, Effects of spatial scale on stomatal control of transpiration. *Agr. Forest Meteorol.* **54** (1991) 279–301.

R.E. Mickle, N.J. Cook and A.M. Hoff, The Askervein hill Project: Vertical profiles of wind and turbulence, *Boundary-Layer Meteorol.*, **43** (1988) 143–169.

C.H. Moeng and J.C. Wyngaard, Statistics of conservative scalars in the convective boundary layer, *J. Atmospheric. Sci.* 41 (1984) 3161–3169.

J.L. Monteith, Evaporation and the environment. *Symp. Soc. Exp. Biology* **19** (1965) 205–234.

R.E. Morris, T.C. Meyers, *User's guide for the urban Airshed Model, Volume 1: User's Manual for UAM(CB-IV).* EPA-450/4–90–007A, U.S. Environmental Protection Agency, Research Triangle Park, NC (1990).

P.J. Mulhearn and J.J. Finnigan, Turbulent flow over a very rough, random surface, *Bound. Layer Meteorol.* **15** (1978) 109–132.

National Ambient Air Quality Standards (NAAQS), 1997, U.S. Environmental Protection Agency

K. Nagel, S. Rasmussen and C.L. Barrett, Network Traffic as a Sel-Organized Critical Phenomena, LA-UR 96–659, Los Alamos National Laboratory, USA (1996).

C.J. Nappo, Sporadic breakdowns of stability in the PBL over simple and complex terrain, *Boundary-Layer Meteorol.* **54** (1991) 69–87.

F.T.M. Nieuwstadt and R.A. Brost. The decay of convective turbulence, *J. Atmospheric. Sci.* **43** (1986) 532–546

D.O. Oberdorster, R.M. Gelein, J. Ferin and B. Weiss, Association of particulate air pollution and acute mortality; Involvement of ultrafine particles. *Inhal. Toxicology* **7** (1995) 111–124.

T.R. Oke and F.G. Hannell, The form of the urban heat island in Hamilton, Canada. In: *Urban Climates*, WMO Tech. Note 108, No. 108 (1970) pp. 113–126.

T.R. Oke, The surface energy budgets of urban areas. Presented at the WMO Tech. Conf. on Urban Climat. and its Appl., with Special Regard to Tropical Area, Mexico City, Nov. 26–30 (1984).

R.T. Oke, The surface energy budget of urban areas. In: *Modeling the Urban Boundary Layer*, Am. Meteorol. Soc. (1987) pp. 2–51.

T.R. Oke, The heat island of the urban boundary layer: Characteristics, causes and effects. In: J.E. Cermak, A.D. Davenport, E.J. Plate, and D.X. Viegas (eds.) *Wind Climate in Cities*, pp. 801–807, NATO ASI Series E, Vol. 277, Kluwer Academic (1995) pp. 801–807.

M.K. O'Rourke *et al.*, Building materials and importance of house dust mite exposure in the Sonoran Desert, Proceedings of the 6th In. Conf. On Indoor Air Quality, Helsinki (1993) pp. 4,155–160.

Y.D. Oyha, E. Neff and R.N. Meroney, Turbulence structure in a stratified boundary layer under stable conditions, *Boundary-Layer Meteorol.* **83** (1997) 139–161.

A.C. Petersen, B. Cees, H. van Dop and P.G. Duynkerke, Mass-flux characteristics of reactive scalars in the convective boundary layer, *J. Atmospheric. Sci.* **56** (1999) 37–56.

R.A. Pielke, *Mesoscale Meteorology Modeling*, Academic Press (1984) pp. 612.

R.A. Pielke, W.R. Cotton, R.L. Walko, C.J. Tremback, W.A. Lyons, L.D. Grasso, M.E. Nicholls, M.D. Moran, D.A. Wesley, T.J. Lee and J.H. Copeland, A comprehensive meteorological modeling system – RAMS, *Meteorol. Atmospheric. Phys.*, **49** (1992) 69–91.

M. Piper, J.C. Wyngaard, W.H. Snyder and R.E. Jr. Lawson, Top-down, bottom-up diffusion experiments in a water convection tank, *J. Atmospheric. Sci.* **52** (1995) 3607–3619.

A.D. Pendwarden and A.F.E. Wise, Wind environment around buildings, Building research Establishment Report, Her Majesty's Stationery Office, London, U.K. (1975) p. 52.

J.M. Plaza, M. Pujadas and B. Artinano, Formation and transport of the Madrid ozone plume. *J. Air & Waste Man. Assoc.* **47** (1997) 766–774.

J.S. Puttock and J.C.R. Hunt, Turbulent diffusion from sources near obstacles with separated wakes–part I, and eddy diffusivity model, *Atmospheric. Environ.* **13** (1979) 1–13.

Y. Qin and S.C. Kot, Dispersion of vehicular emission in street canyons, Guangzhou City, South China (P.R.C.), *Atmospheric. Environ.* **27B** (1993) 283–291.

M.R. Raupach, Influences of local feedback on land-air exchanges of energy and carbon. *Global Change Bio.* **4** (1998) 447–494.

M.R. Raupach and J.J. Finnigan, Single-layer models of evaporation from plant canopies are incorrect but useful, whereas multi-layer models are correct but useless: discussion. **Australian J. Plant Phys. 15** (1988) 705–716.

M.R. Raupach and A.S. Thom, Turbulence in and above plant canopies, *Ann. Rev. Fluid Mech.*, **13** (1981) 97–129.

S. Rafailidis, Influence of building areal density and roof shape on the wind characteristics above a town. *Bound. Layer Meteorol.* **85** (1997) 255–271.

S. Rafailidis, Wind induced flows above buildings and inside street canyons: Building density, roof shape and arrangement effects. *J. Fluid Mech.*, (2001) submitted.

S. Rafailidis and M. Schatzmann, Physical Modeling of car exhaust dispersion in urban street canyons – The effect of Slanted Roofs. In: S.E. Gryning and F. Schiermeier (eds.), *Air Pollution Modelling and its Applications XI*, Plenum Press, New York, (1996) pp. 653–654.

L.W. Richards, C.L. Blanchard and D.L. Blumenthal (eds.), Navajo Generating Station visiblity final report. Rep. STI-90200–1124–FR, Sonoma Technology. Inc., Santa Rosa, CA (1991) 408 pp. [Available from Salt River Project, P. O. Box 52025, Phoenix, AZ 85072–2025].

J.H. Schreffler, Detection of centripetal heat island circulations from tower data in St. Louis, *Bound. Layer Meteorol.* **15** (1978) 229–242.

Y. Sasaki, Some basic formalisms in numerical variables analysis, *Mon. Wea. Rev.* **98** (1970) 875–883.

C. Sherman, A mass-consistent model for wind fields over complex terrain, *J. Appl. Meteorol.* **17** (1978) 312–319.

E.D. Siggia, High Rayleigh number convection, *Ann. Rev. Fluid Mech.* **26** (1994) 137–168.

E.J. Simpson, *Gravity currents in the environment and the laboratory*, Cambridge University Press (1997).

W.S. Smith, J.M. Reisner, D.S. Decroix, M.J. Brown, R.H. Lee, S.T. Chan, and D.E. Stevens, A CFD model intercomparison and validation using high resolution wind tunnel data, 11th *Conference on the Applications of Air Pollution Meteorology with A& WMA*, 9–14 January, Long Beach, CA. (2000) 41–46.

W.H. Snyder, L.H. Khurshudyan, I.V. Nekrasov, R.E. Jr. Lawson and R.S. Thompson, Flow and dispersion of pollutants within two-dimensional valleys, *Atmospheric. Environ.* **25** (1990) 1347–1375.

Z. Sorbjan, Decay of convective turbulence revisited, *Boundary-Layer Meteorol.* **82** (1997) 501–515.
E.J. Strang and H.J.S. Fernando, Entrainment and mixing stratified shear flows, *J. Fluid Mech.* (2000) In Press.
R.B. Stull, *An introduction to boundary layer meteorology*, Kluwer Academic Publisher (1988) pp. 666.
P.A. Taylor, R.E. Mickle, J.R. Salmon and H.W. Teunissen, The Kettles Hill experiment-site description and mean flow results, Internal Report Aqrb-83–0020L, Atmospheric. Environ. Service, Downsview, Ont., Canada (1983).
A.A. Townsend, Self-preserving flow inside a turbulent boundary layer, *J. Fluid Mech.* **22** (1965) 773–797.
A.A. Townsend, The flow in a turbulent boundary layer after a sudden change in surface roughness, *J. Fluid Mech.*, **26** (1966) 255–266.
D.B. Turner, Atmospheric dispersion modeling, a critical review, *J. Air Pollut. Control Assoc.* **29** (1979) 502–519.
Z. Uchijima and J.L. Wright, An experimental study of air flow in a corn plant air-layer, *Bull. Natl. Inst. Agric. Sci. (Jpn)* **Ser.A11** (1964) 19–65.
I. Uno, H. Ueda and S. Wakamatsu, Numerical modeling of the nocturnal urban boundary layer, *Boundary-Layer Meteorol.* **49** (1989) 77–98.
A. Urano, T. Ichinose and K. Hanaki, Thermal environment simulation for three dimensional replacement of urban activity, *J. Wind Eng. Ind. Aero.* **81** (1999) 197–210.
User's guide to CAL3QHC version 2.0, *A modeling methodology for predicting pollutant concentrations near roadway intersections*, EPA-454/R-92–006, U.S. Environmental Protection Agency (1994).
K.D. Van der Hout, H.P. Baars and N.J. Duijm, Effects of Buildings and Trees on Air Pollution by Road Traffic, T.N.O. Div. Of Technology for Society, P.O. Box 217, NL-2600 AE Delft, Netherlands, 6 (1989)
I. Vergeiner and E. Dreiseitl, Valley winds and slope winds-observations and elementary thoughts, *Meteorol. Atmospheric. Phys.* **36** (1987) 264–286.
J.X.L. Wang and J.K. Angell, Air stagnation climatology for the United States (1948–1998). NOAA/Air Resources Laboratory ATLAS No. 1 (1999).
Y.P. Wang, R. Leuning, A two-leaf model for canopy conductance, photosynthesis and partitioning of available energy I: Model description and comparison with a multi- layered model. *Agr. Forest Meteorol.* **91** (1998) 89–111.
A.H. Weber and R.J. Kurzeja, Nocturnal planetary boundary layer structure and turbulence episodes during the Project STABLE field program, *J. Appl. Meteorol.* **30** (1991) 1117–1133.
C.D. Whiteman, Morning transition tracer experiments in a deep narrow valley, *J. Appl. Meteorol.* **28** (1989) 625–635.
C.D. Whiteman, Observations of thermally developed wind systems in mountainous terrain. In: W. Blumen (Ed.), Atmospheric Processes Over Complex Terrain, Meteorol. Monogr. 23 (45), *American Meteorology Society*, Boston, Massachusetts (1990) pp. 5–42.
C.D. Whiteman and S. Barr, Atmospheric mass transport by along-valley wind systems in a deep Colorado Valley, *J. Climate Appl. Meteorol.* **25** (1996) 1205–1212.
C.D. Whiteman and J.C. Doran, The relationship between overlying synoptic-scale flows and winds within a valley, *J. Appl. Meteorol.* **32** (1993) 1669–1682.
C.D. Whiteman, T.B. McKee and J.C. Doran, Boundary layer evolution within a canyon land basin, Part I: Mass, heat and moisture budgets from observations, *J. Appl. Meteorol.* **35** (1996) 2145–2161.
D.J. Wilson and R.E. Britter, Estimates of building surface concentrations from nearby point sources, *Atmospheric. Environ.* **16** (1982) 2631–2646.
K.K. Wong and R.A. Dirks, Mesoscale perturbations on airflow in the urban mixing layer, *J. Appl. Meteorol.* 17 (1978) 677–688

S.C. Wong, I.R. Cowan, G.D. Farquhar, Stomatal conductance correlates with photosynthetic capacity, *Nature* **282** (1979) 424–426.

P.H. Wood, Calculation of the neutral wind profile following a large step change in surface roughness, *Q. J. Roy. Meteorol. Soc.* **104** (1978) 383–392.

M. Xue, K.K. Droegemeier, V. Wong, A. Shapiro and K. Brewster, *ARPS Version 4.0 user's guide* (1995) pp. 380.

T. Yamada, A numerical simulation of nocturnal drainage flow, *J. Meteorol. Soc. Japan* **59** (1981) 108–122.

T. Yamada, Building and terrain effects in a mesoscale model, 11th *Conference on the Applications of Air Pollution Meteorology with A& WMA*, 9–14 January, Long Beach, CA (2000) pp. 215–220.

M.M. Zdravkovich, Interstitial flow in tube arrays: A series of formidable paradoxes. In: R.J. Perkins and S.E. Belcher, eds., *Flow and Dispersion Through Groups of Obstacles* Clarendon Press (1997) pp. 141–142.